Large-Eddy Simulation of Combustion Noise: Towards Noise Predictions in Complex Geometry

M. Ihme, A.L. Birbaud, A. Giauque, H. Pitsch
Department of Mechanical Engineering
Stanford University

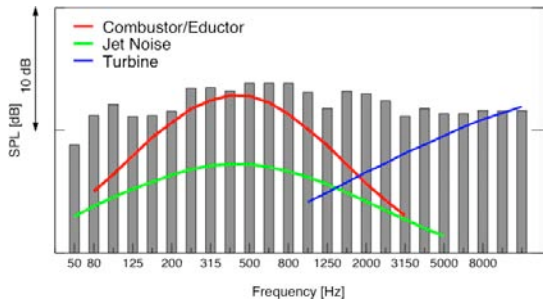

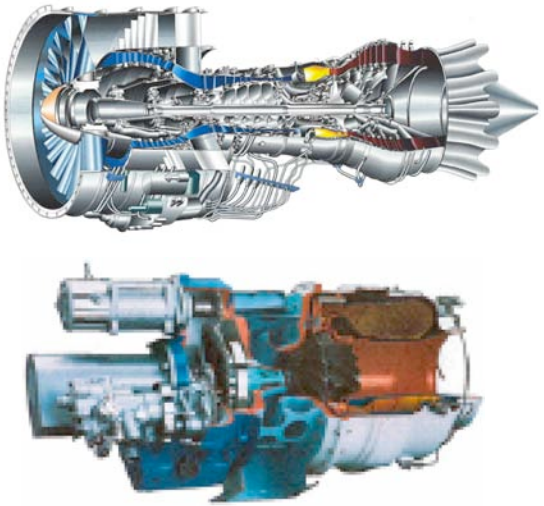

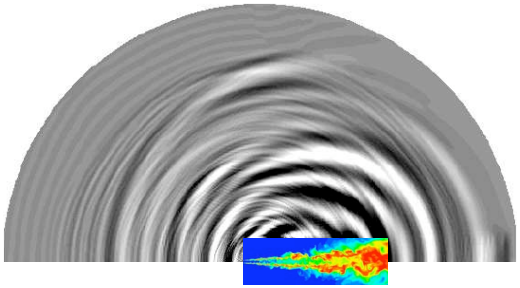

Funding by NASA

Noise Emissions from Aircraft Engines

- Fundamental understanding of mechanisms for generation and propagation of combustion generated noise, including direct and indirect combustion noise
- Enable and perform predictive simulations of noise emissions from aircraft engines
- Develop LES methodology for accurate coupled predictions of combustion noise in combustor and turbine

- Challenges
  - Reactive flow modeling
  - Combustor/turbine coupling
  - Accuracy
  - Complex geometry

Requirements

- High-fidelity CFD basis:
  - Large-eddy simulation solver
    - Accurate enough to compute noise
    - Complex geometry
  - Advanced physical models to better capture reactive flow field
    - Accurate computation of density (no filtering!)
  - Environment for accurate code coupling

Noise Predictions in Complex Geometry

- First option: Fully Compressible
  - Requires high numerical accuracy
  - Could be feasible in combustor LES
    - But sufficient accuracy can hardly be achieved on unstructured meshes
  - Turbine computed with RANS
    - LES too expensive
  - RANS turbomachinery solvers compressible, but not accurate enough

Noise Predictions in Complex Geometry

- Second option: Acoustic analogy
  - Base flow + acoustic analogy
  - Base flow could be LES (combustor) or RANS (turbine)
  - Only evaluation of sources and acoustic analogy solver need to be very accurate
  - Different acoustic analogies possible
    - Lighthill
    - Phillips
    - Lilley
    - Goldstein

Acoustic Analogies

- Lighthill's acoustic analogy
  - Recast Navier-Stokes equations into
    Wave equation in non-moving medium = Sources
  - Decoupling of acoustic source and acoustic variables
  - Limited applicability
- Goldstein's Generalized Analogy
  - Recast Navier-Stokes equations into
    Linearized isentropic NS = Sources
  - Linearization about arbitrary base flow
  - No assumptions until source terms are closed
  - Can handle refraction, reflection, indirect noise

Overview

- Simple geometry: Open flames
  - CLES/CAA model using Lighthill's analogy for noise emissions from open flames
    - Direct noise
    - Assess combustion modeling for noise predictions
    - Assess numerical accuracy
    - Validation
- Towards noise simulations in complex geometry
  - Strategy
  - Compressible CLES for noise predictions in confined geometries
    - Compressible algorithm
    - What is the required accuracy?
  - CLES/Goldstein's acoustic analogy for predictions of direct and indirect noise in combustor and turbine
    - Formulation and numerical accuracy

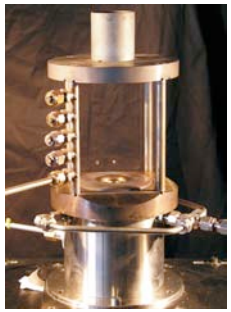

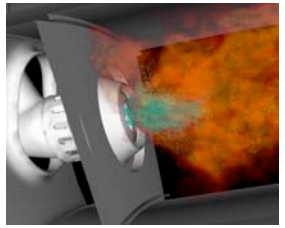

CLES/CAA Model to Predict Noise Emissions from Open Flames

- Development of methodology for prediction of combustion-generated noise
  - Noise emissions only for open flames
- Test accuracy of combustion model
  - Accuracy of unsteady scalar predictions
  - Accuracy of numerical implementation
  - Lighthill's acoustic analogy for prediction of radiated sound field
- Use well-characterized DLR flame for model validation
  - Analysis of acoustic source terms

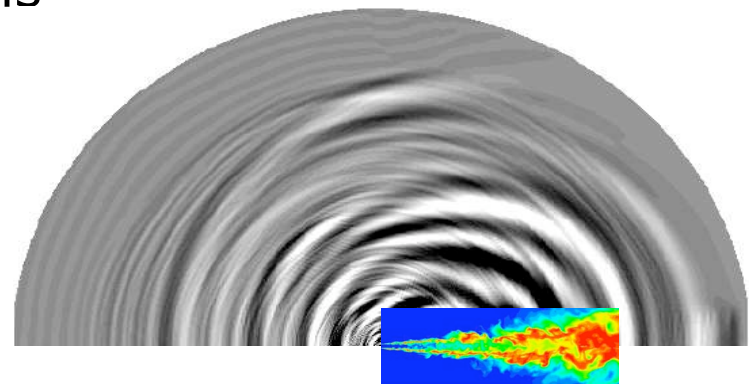

Combustion Model

- Flamelet/Progress Variable model (Pierce & Moin 2004, Ihme et al. 2004)
- Solve transport equations for mixture fraction and reaction progress variable
- Chemical source term closed from flamelet table generated from solution of flamelet equations and presume PDF
- Parameterization by mixture fraction Z and reaction progress variable C

$$\widetilde{\dot{\omega}}_C = \widetilde{\dot{\omega}}_C(\widetilde{Z}, \widetilde{Z''^2}, \widetilde{C})$$

- Important
  - Dependence on Z and C
  - Tabulation

Pierce & Moin, J. Fluid Mech, , 2004
Ihme, Cha & Pitsch, Proc. Comb. Inst., 30, 2004

Mathematical Method

- Combustion LES
  - Use low-Mach-number, variable density LES-formulation
- Lighthill's acoustic analogy
  - Source terms active only in LES region

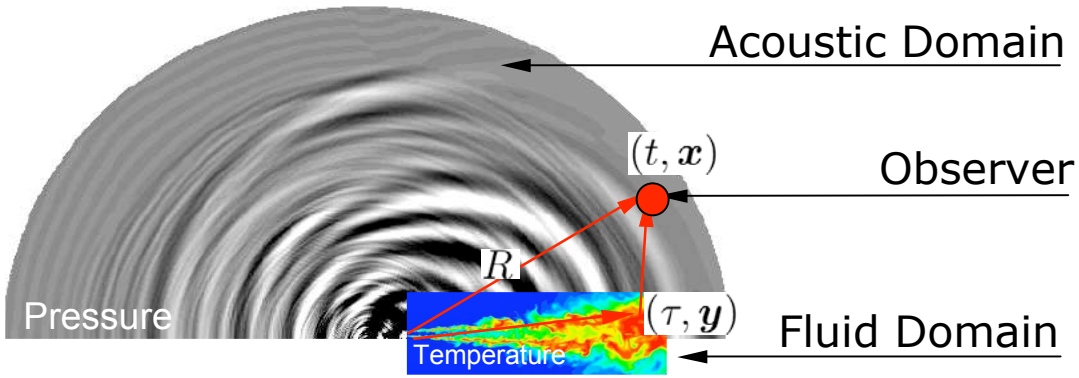

Mathematical Method

- Use Lighthill's acoustic analogy for prediction of far-field noise (Lighthill 1952)

$$\left\{\mathrm{M}^2\partial_\tau^2 - \Delta\right\} p' = \nabla\cdot\nabla\cdot\left(\rho\boldsymbol{uu} - \frac{1}{\mathrm{Re}}\underline{\underline{\sigma}}\right) - \partial_\tau^2\underbrace{\left((\rho-1) - \mathrm{M}^2 p'\right)}$$

- Numerical accuracy of source term evaluation requires model for excess density
- Using FPV model, excess density can consistently be expressed by first-order source terms
- Simplified wave equation (neglect viscous and diffusive contributions, pressure fluctuations) (Ihme et al. 2006)

$$\left\{\mathrm{M}^2\partial_\tau^2 - \Delta\right\} p' = \nabla\cdot\nabla\cdot\underbrace{(\rho\boldsymbol{uu})}_{\underline{\underline{T}}_{\mathrm{R}}} - \partial_\tau\nabla\cdot\underbrace{((1-\rho)\boldsymbol{u})}_{\boldsymbol{F}_{\mathrm{M}}} - \mathrm{Da}\partial_\tau\underbrace{\left(\frac{1}{\rho}\partial_C\rho\omega_C\right)}_{Q_{\mathrm{H}}}$$

Ihme, Bodony, & Pitsch, AIAA paper 2006-2614

Far-field Source Term Contribution

- Acoustic source term scaling
  - Total acoustic power: $P_{\mathrm{ac}} = \mathrm{M}\,\overline{p'^2}$
  - Rate of chemical and kinetic energy:

$$\dot{E}_{\mathrm{in}} = \dot{m}\left\{h + \mathrm{Ec}(p/\rho + U_{\mathrm{J}}^2/2)\right\}$$

Reynolds stress term	$\underline{\underline{T}}_{\mathrm{R}} = \rho \boldsymbol{u}\boldsymbol{u}$	$\dfrac{P_{\mathrm{ac}}(\underline{\underline{T}}_{\mathrm{R}})}{\dot{E}_{\mathrm{in}}} \propto \mathrm{M}^5$
Momentum fluctuation term	$\underline{F}_{\mathrm{M}} = (1-\rho)\boldsymbol{u}$	$\dfrac{P_{\mathrm{ac}}(\underline{F}_{\mathrm{M}})}{\dot{E}_{\mathrm{in}}} \propto \mathrm{M}^3$
Chemical source term	$Q_{\mathrm{H}} = \dfrac{\omega_C}{\rho}\dfrac{\partial \rho}{\partial C}$	$\dfrac{P_{\mathrm{ac}}(Q_{\mathrm{H}})}{\dot{E}_{\mathrm{in}}} \propto \mathrm{Da}\,\mathrm{M}$

$\Rightarrow$ Chemical source term is dominant source of sound in open turbulent flames (Da=0.64, M=0.12)

Combustion-Generated Noise

- Numerical implementation
  - Use Lighthill's integral formulation (free-space Green's function)
  - Transfer spatial derivatives to Green's function using integration by parts
  - Solve far-field pressure in Fourier space

$$\widehat{p'}(\omega, \boldsymbol{x}) = \frac{1}{4\pi} \iiint_{\Omega_{\mathcal{F}}} \frac{\exp\{-\mathrm{i}\omega \mathrm{M}|\boldsymbol{x}-\boldsymbol{y}|\}}{|\boldsymbol{x}-\boldsymbol{y}|} \widehat{\gamma}_a(\omega, \boldsymbol{y}) \mathrm{d}\boldsymbol{y}$$

$$\widehat{\gamma}_{\mathrm{a}} = \omega^2 \underline{\underline{\kappa}} : \underline{\underline{\widehat{T}}}_{\mathrm{R}} + \omega^2 \underline{\lambda} \cdot \underline{\widehat{F}}_{\mathrm{M}} + \omega \mu \widehat{Q}_{\mathrm{H}}$$

Directional cosine

Experimental Configuration

- Application
  - Use well-characterized non-premixed jet flame (DLR flame A)
    - N_2-diluted CH_4/Air-flame
    - Re = 15,200 (U_b=42.2 m/s)
    - Nozzle diameter: D=8 mm
    - Fuel-stream: 22.1% CH_4, 33.2% H_2, 44.7% N_2
  - Comprehensive data set
    - Scalar point measurements for species
    - Velocity measurements
    - Far-field sound pressure level

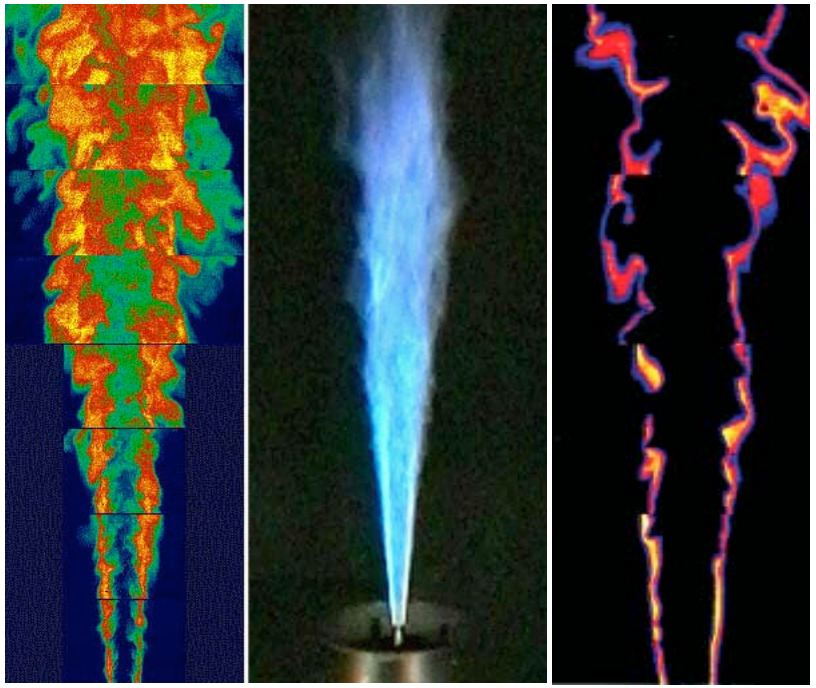

Temperature OH

Flow Field: Centerline Profiles

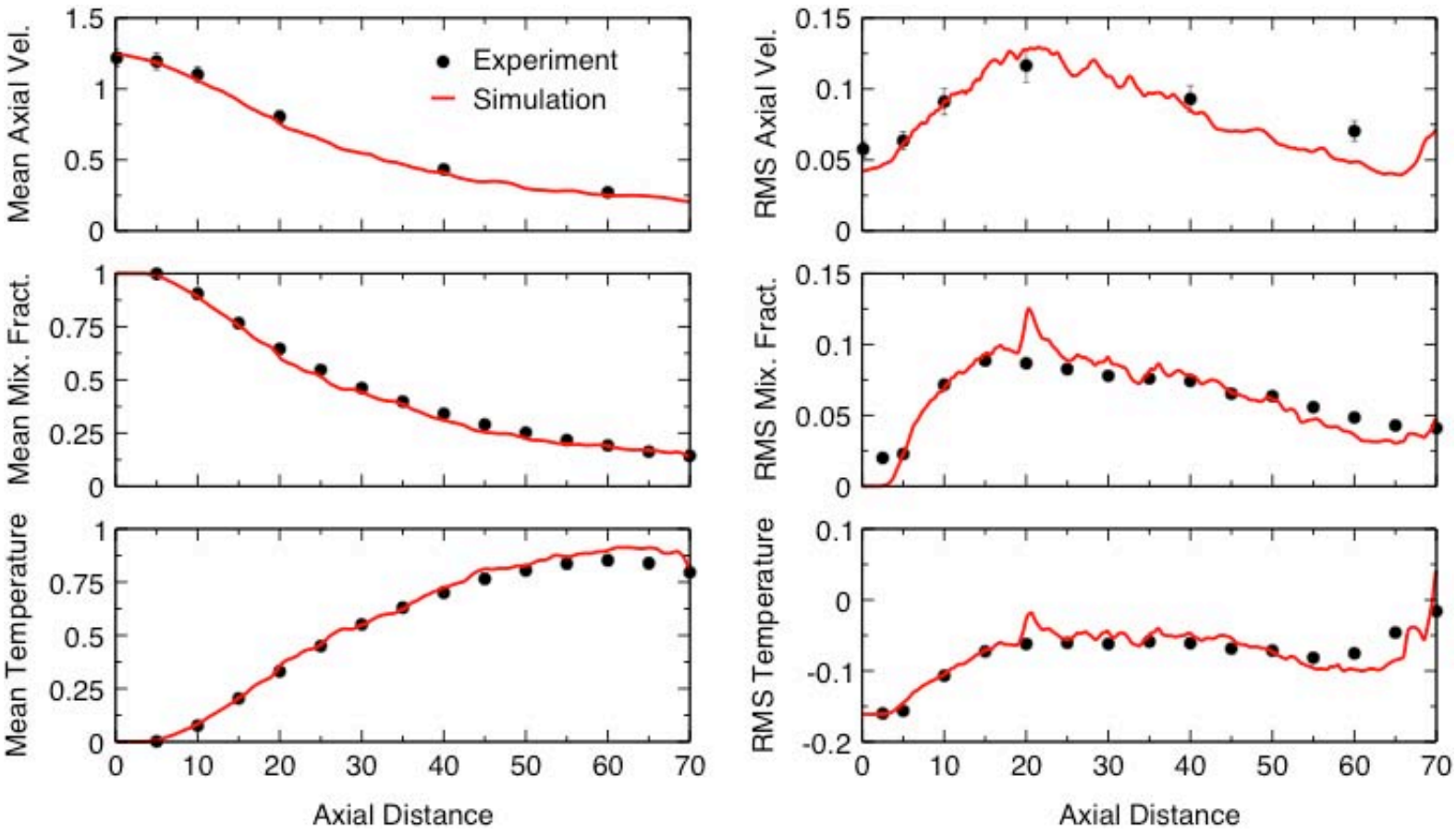

Flow Field: Radial Profiles

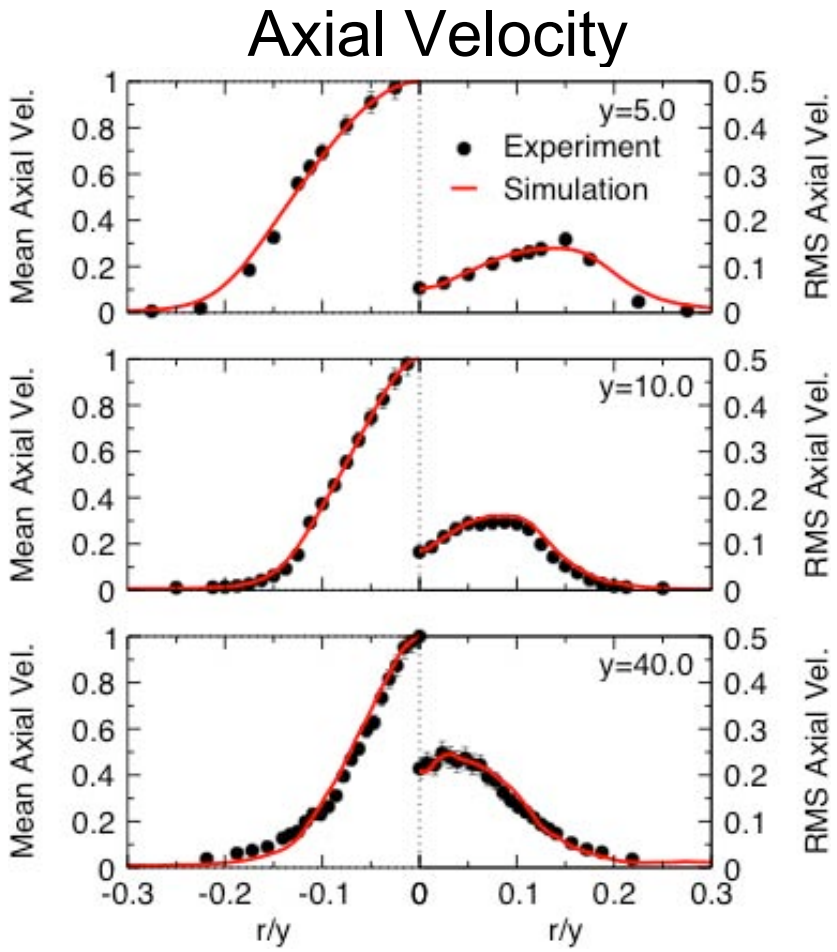

⇒ Overall good agreement between simulation and experiment for flow field quantities

Chemistry Model

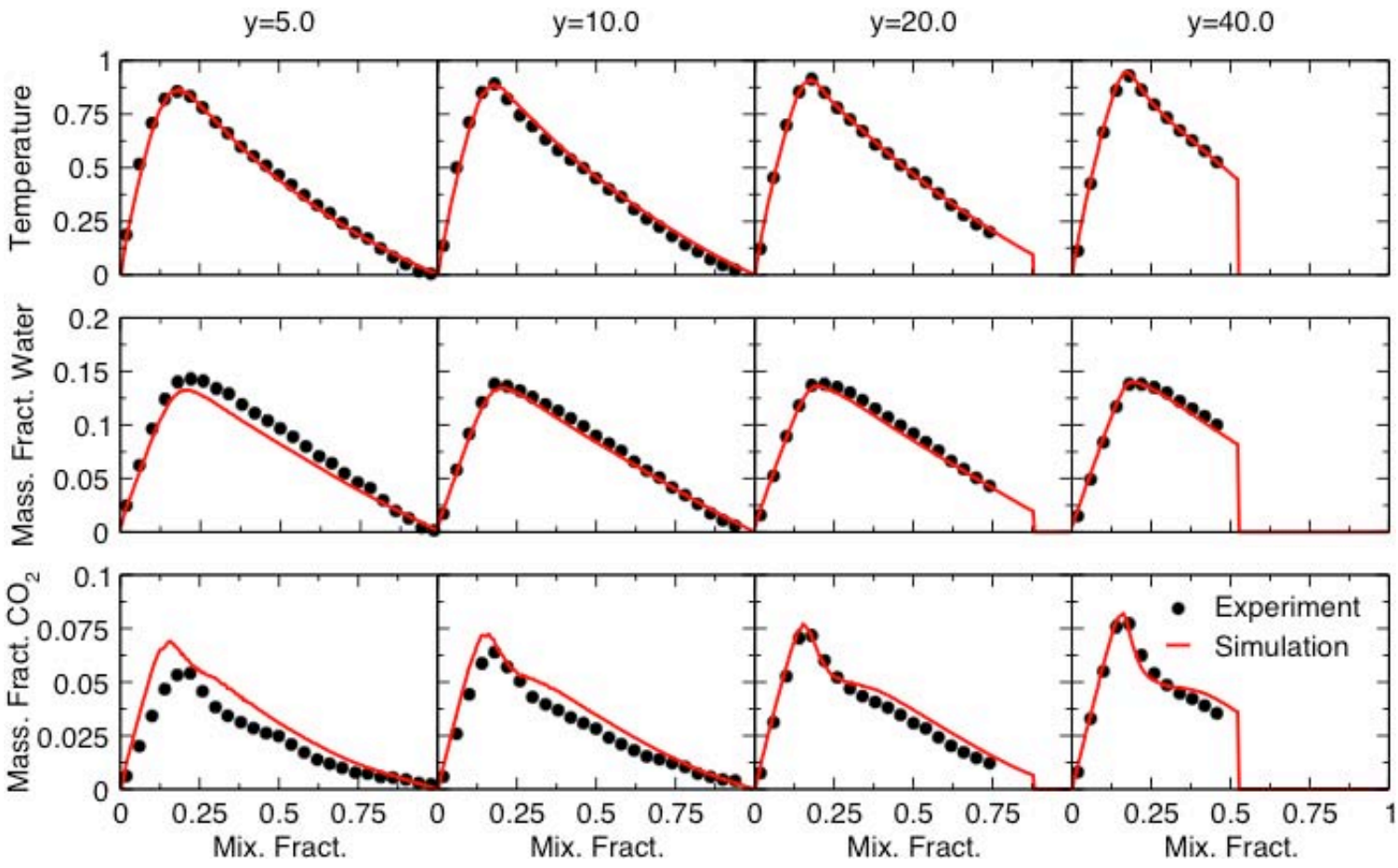

⇒ Good agreement between simulation and experiment for temperature and major chemical species

Spurious Noise Sources

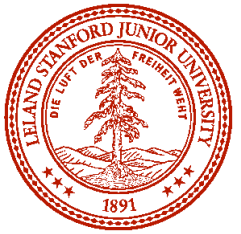

- Numerical method and combustion model introduce spurious noise sources polluting acoustic results

- Noise sources
  - Combustion model and interpolation technique
  - Limited temporal and spatial resolution
  - Subgrid scale modeling
  - Numerical methods

Spurious Noise Sources

- Combustion model employs chemistry tabulation with tri-linear interpolation in $(\tilde{Z}, \widetilde{Z''^2}, \tilde{C})$-space
- Interpolation and resolution introduces spurious noise at high frequencies

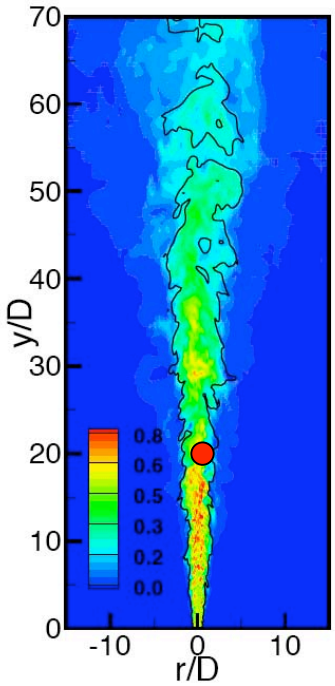

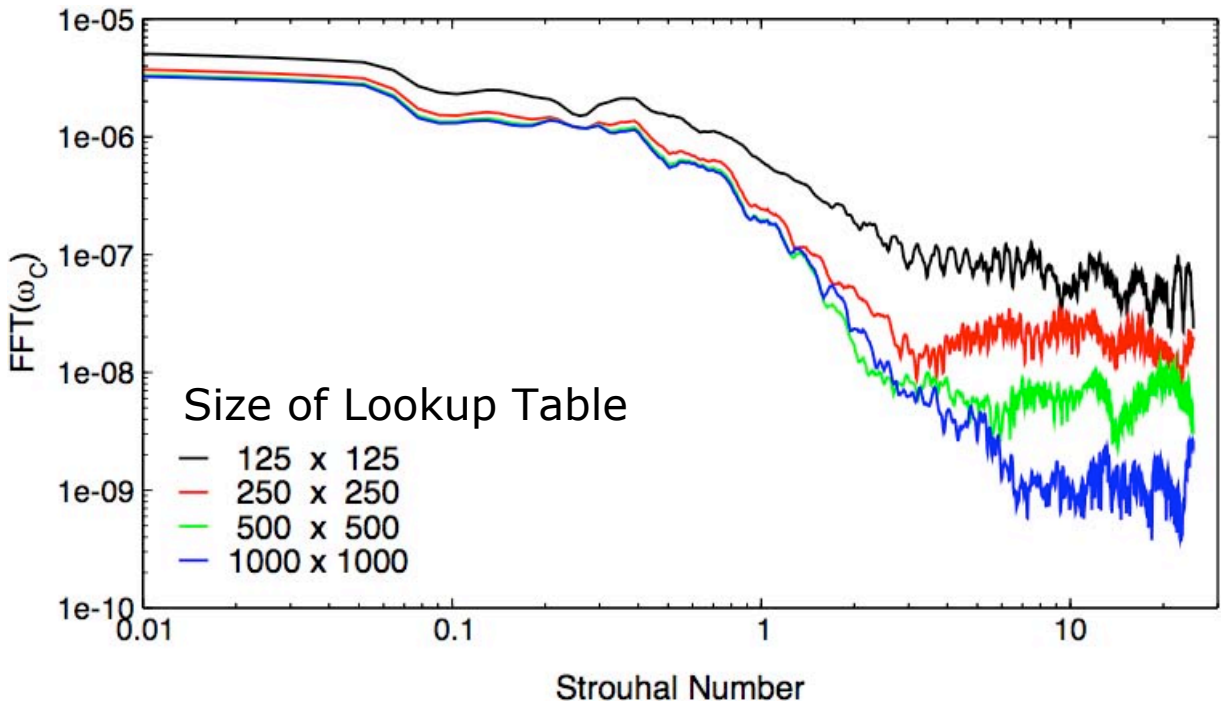

Tabulated Chemistry

Two errors (Shunn and Ham, 2006)

- Tri-linear interpolation
- Tabulated quantities might vary more strongly than parameters

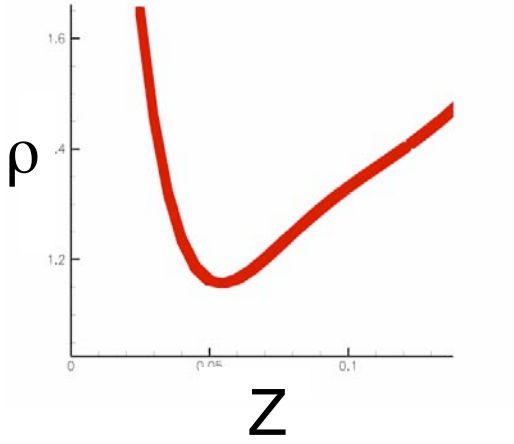

Finite volume scheme

$$\frac{1}{\Delta x}\int \rho\phi\, dx = \rho_p\phi_p + \frac{\Delta x^2}{24}\left(\phi_p\frac{\partial\rho}{\partial\phi}\frac{\partial^2\phi}{\partial x^2} + \phi_p\frac{\partial^2\rho}{\partial\phi^2}\left(\frac{\partial\phi}{\partial x}\right)^2 + 2\frac{\partial\rho}{\partial\phi}\left(\frac{\partial\phi}{\partial x}\right)^2 + \ldots\right)$$

Error is second order, but these terms can be very large in some regions of the state equation

- Higher accuracy by tetrahedral based integration to evaluate finite volume based value

Shunn & Ham, CTR Research Briefs, 2006

Spurious Noise Sources

- Accuracy can further be improved by employing
  - Tetrahedral integration **(Shunn & Ham, 2006)**
  - Artificial Neural Networks **(Ihme, Marsden & Pitsch, 2007)**

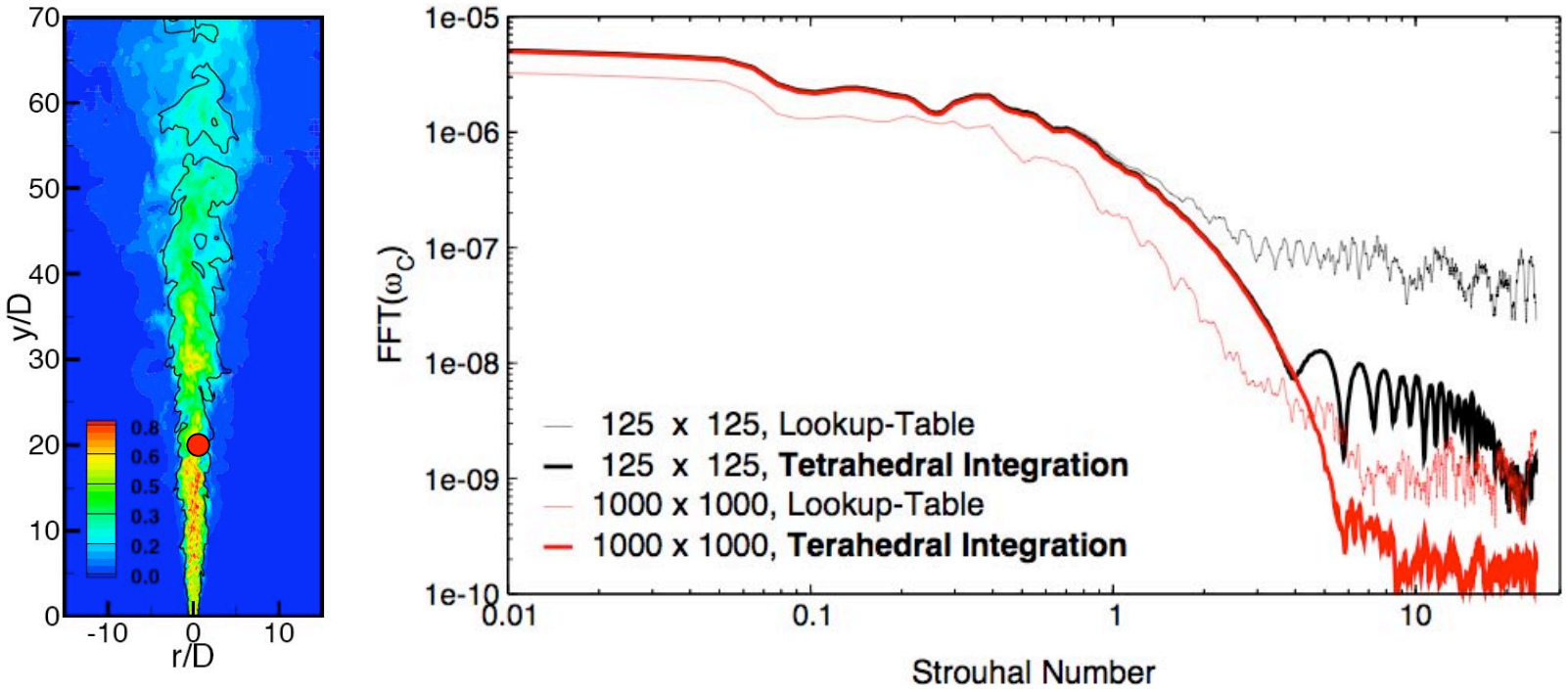

Ihme, Marsden, Pitsch, Neural Networks, 2007

Spurious Noise Sources

- Temporal resolution
  - Sample frequency of acoustic data: $\Delta\tau = 0.04$
  - Nyquist Strouhal number: $St_N = (2\ \Delta\tau)^{-1} = 12.5$

    $\Rightarrow$ Not limiting
- Spatial resolution
  - Critical Strouhal number associated with the advection of acoustic sources

$$\mathrm{St}_a = \frac{\langle \widetilde{\boldsymbol{u}} \rangle (\boldsymbol{y})}{2\Delta y}$$

  - … but $\langle \widetilde{\boldsymbol{u}} \rangle \sim y_1^{-1}$ and $\Delta y \sim y_1$

    $\Rightarrow$ and therefore

$$\mathrm{St}_a \sim \frac{1}{y_1^2}$$

Energy Spectra

- Source term spectra

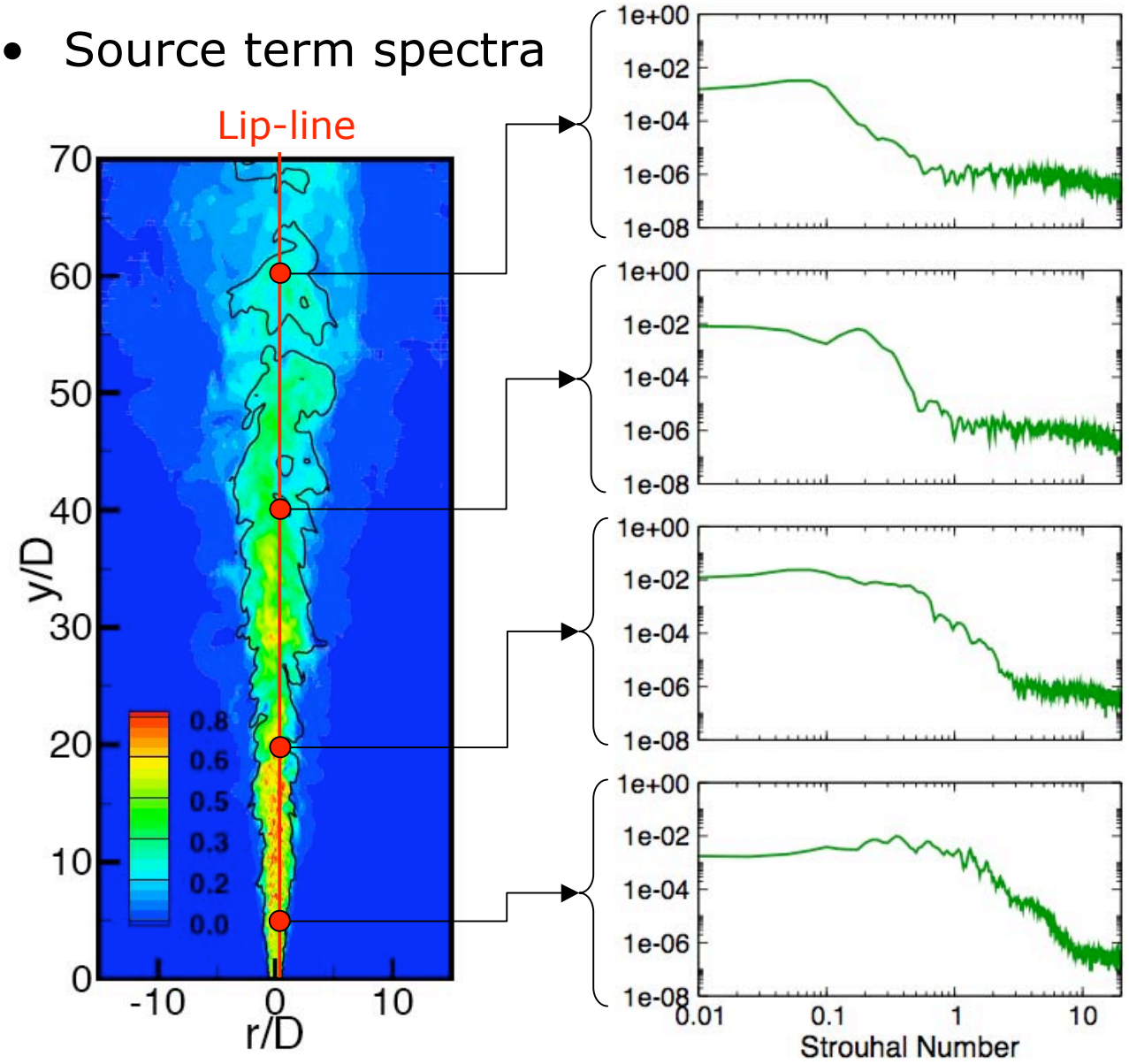

$$\widehat{\widehat{F}}_{\mathrm{M},1} = \widehat{(1-\overline{\rho})\widetilde{u}_1}$$

Energy Spectra

- Source term spectra

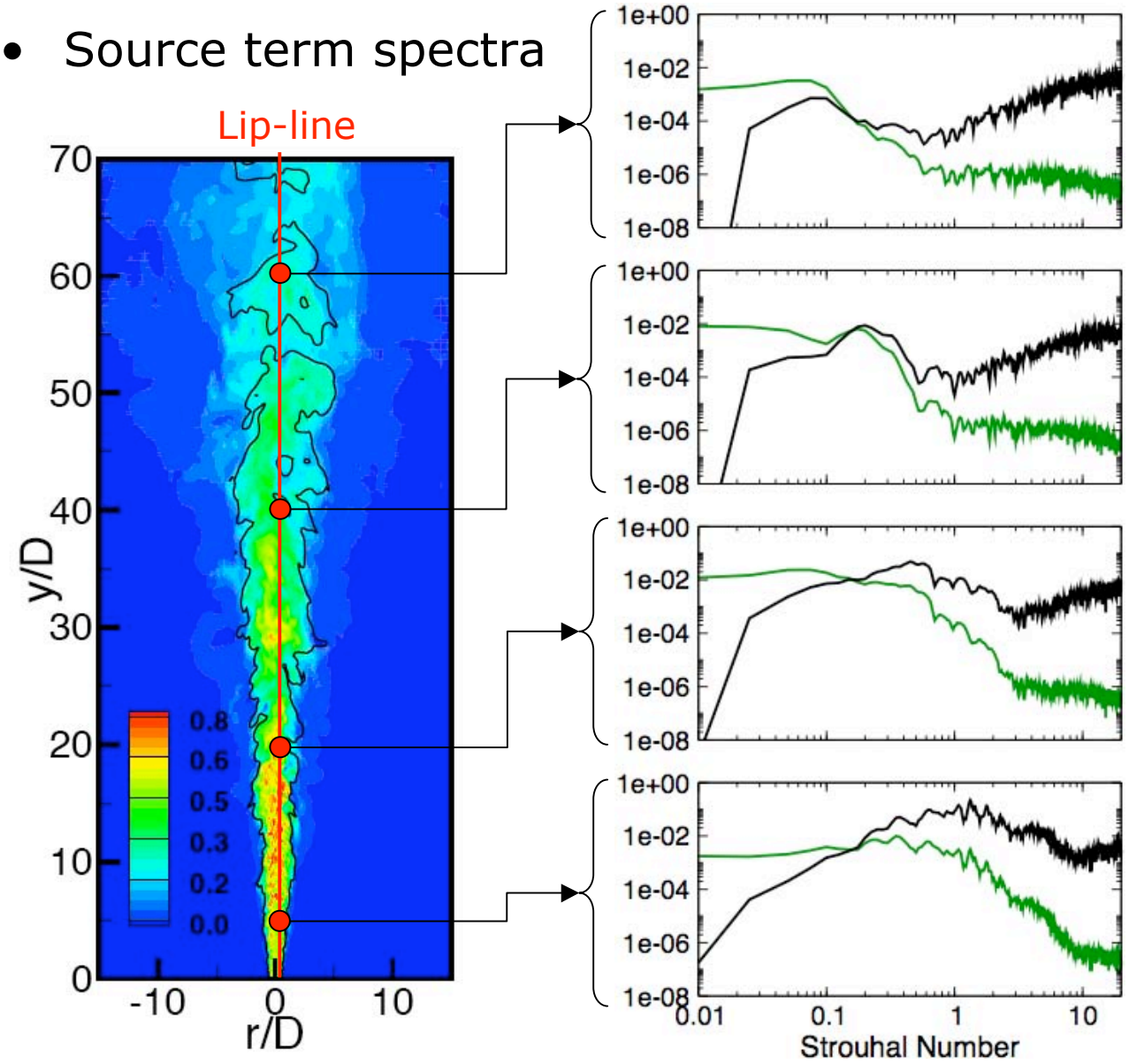

$$\widehat{p}_{F_{\mathrm{M}}} \propto \omega^2 \, \widehat{\overline{F}}_{\mathrm{M},1}$$

$$\widehat{\overline{F}}_{\mathrm{M},1} = \widehat{(1-\overline{\rho})\widetilde{u}_1}$$

Energy Spectra

- Source term spectra

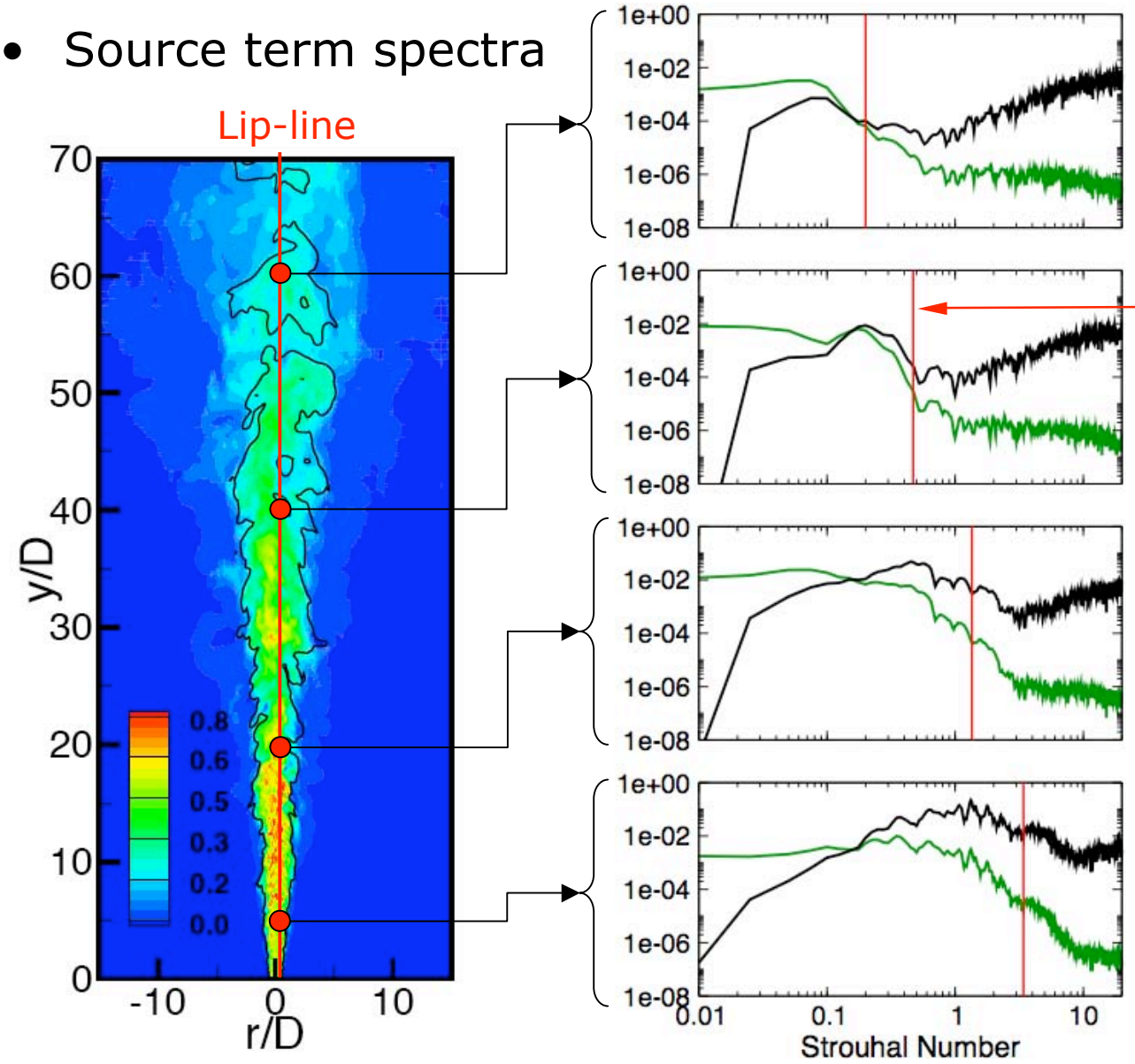

$$\widehat{p}_{F_{\mathrm{M}}} \propto \omega^2 \widehat{\widetilde{F}}_{\mathrm{M},1}$$

$$\widehat{\widetilde{F}}_{\mathrm{M},1} = \widehat{(1-\overline{\rho})\widetilde{u}_1}$$

$$\mathrm{St_c}(\boldsymbol{y}) = \frac{\langle \widetilde{u} \rangle(\boldsymbol{y})}{2\Delta y}$$

- Acoustic sources are convection-dominated
- Filter noise contributions which cannot be supported by numerical grid

Acoustic Source Term Distribution

- Instantaneous acoustic source term distribution
  - LES provides insight into source term structure

$$\overline{T}_{\mathrm{R},11} = \overline{\rho}\widetilde{u}_1\widetilde{u}_1 \qquad \overline{F}_{\mathrm{M},1} = (1-\overline{\rho})\widetilde{u}_1 \qquad \overline{Q}_{\mathrm{H}} = \overline{\rho}\frac{\omega_C}{\rho^2}\frac{\partial \widetilde{\rho}}{\partial C}$$

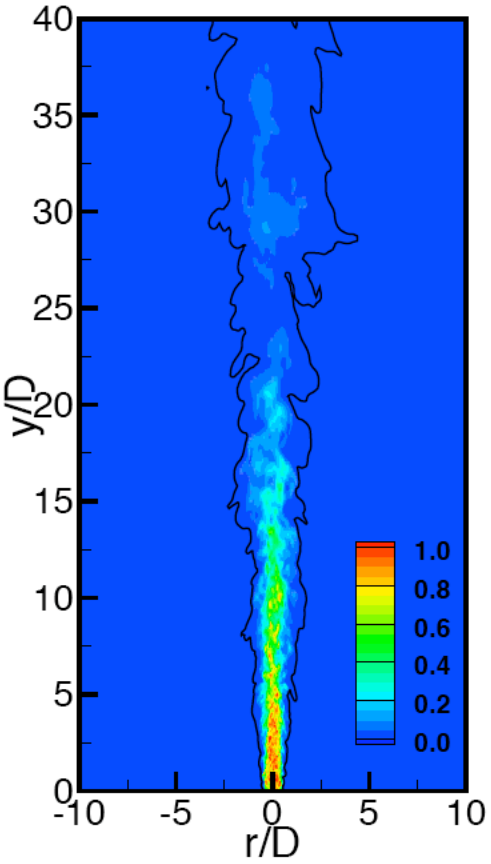

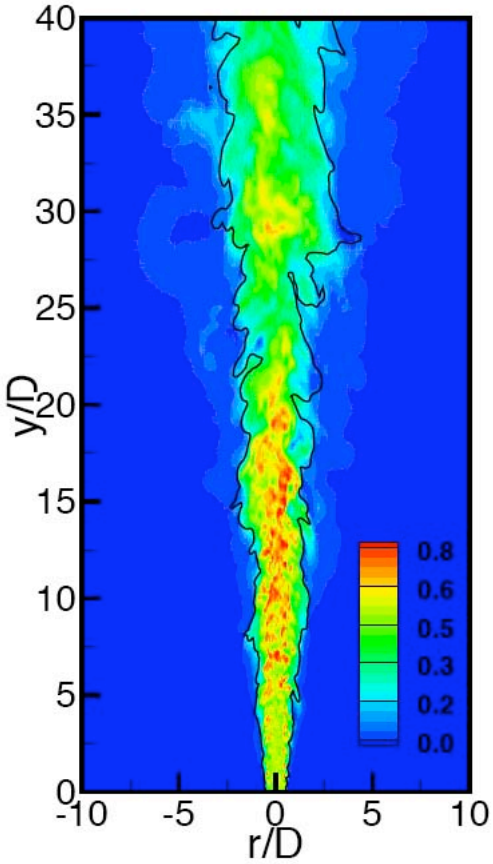

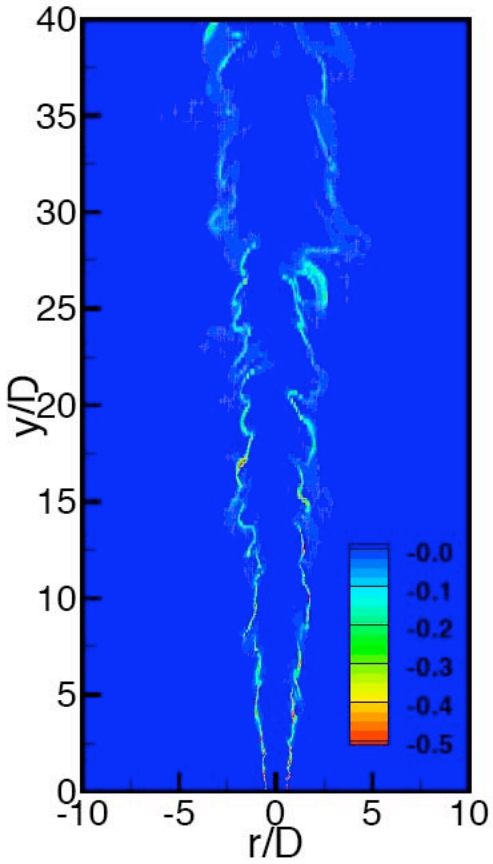

Acoustic Source Term Distribution

- Acoustic source term distribution to far-field pressure at (r=50, x=0)

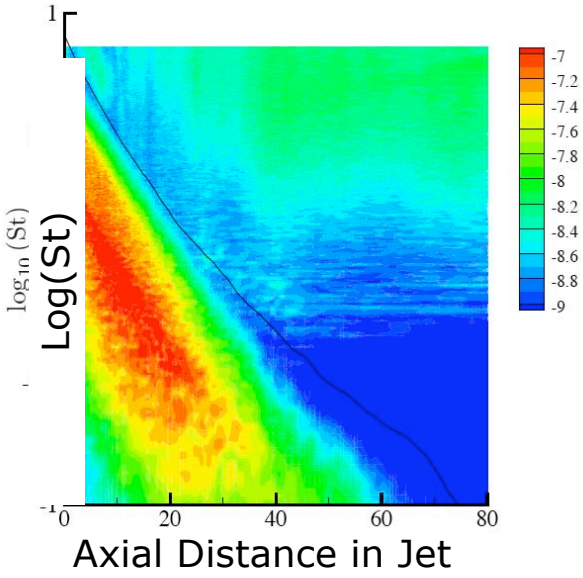

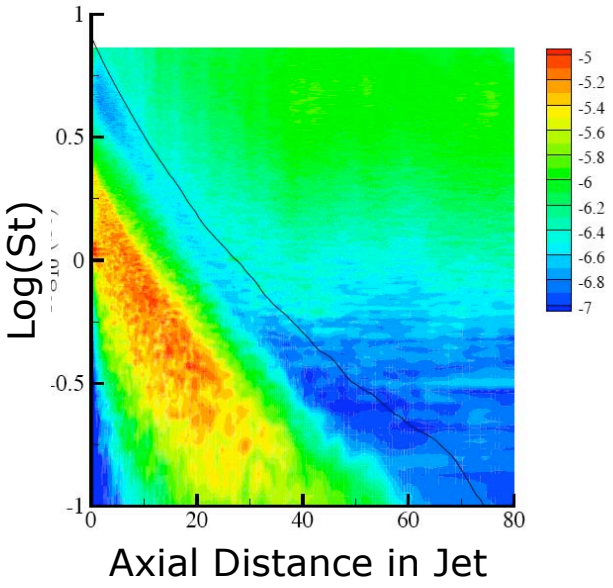

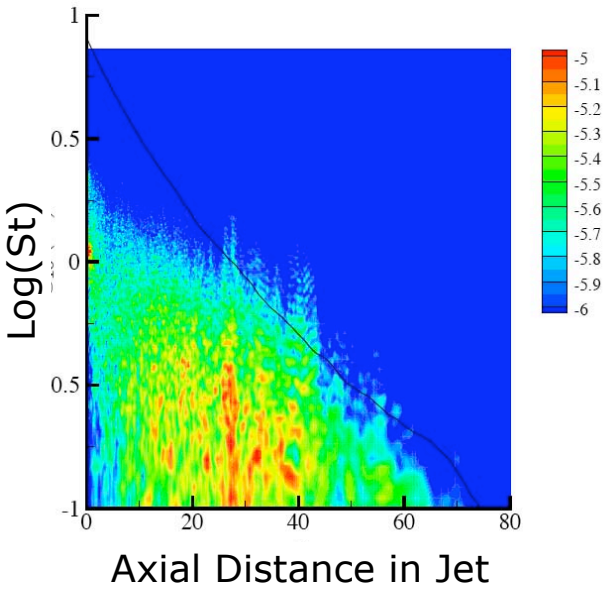

$$\overline{T}_{\mathrm{R},11} = \overline{\rho}\widetilde{u}_1\widetilde{u}_1$$

$$\overline{F}_{\mathrm{M},1} = (1-\overline{\rho})\widetilde{u}_1$$

$$\overline{Q}_{\mathrm{H}} = \overline{\rho}\frac{\omega_C}{\rho^2}\frac{\partial \rho}{\partial C}$$

Acoustic Source Term Distribution

Spurious noise due to Strouhal number limitation of numerical grid

⇒ High pass filter

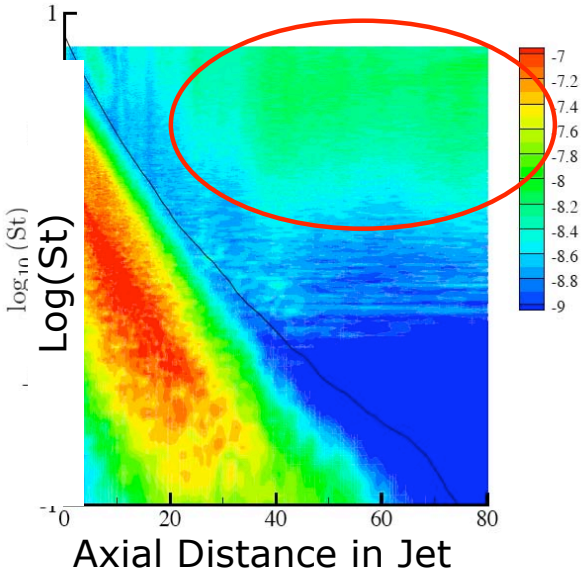

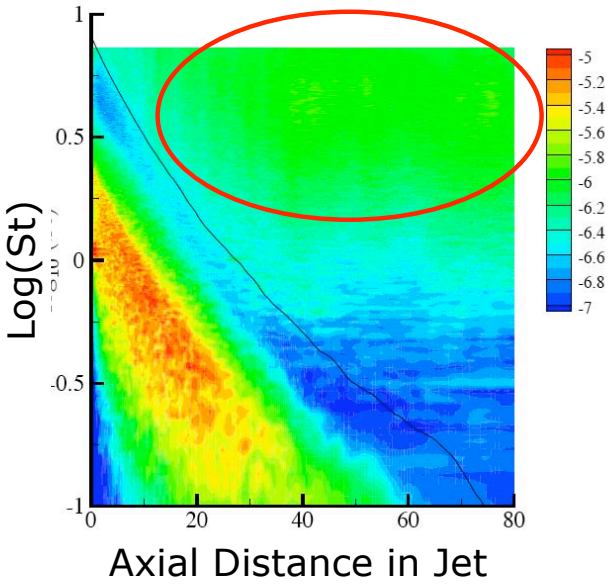

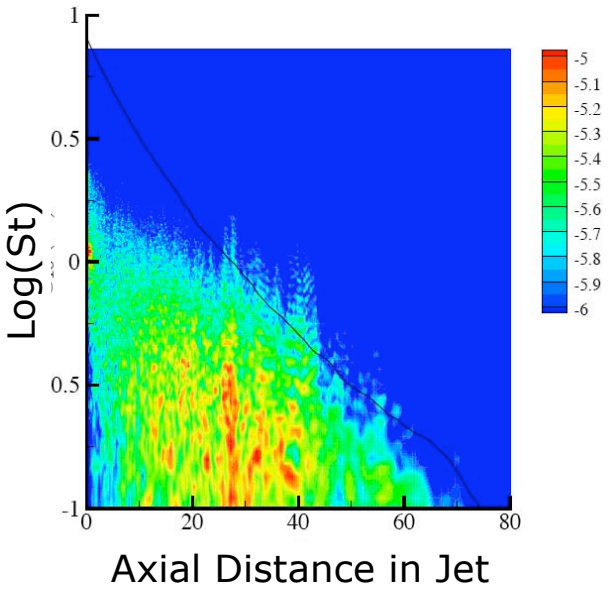

$$\overline{T}_{\mathrm{R},11} = \overline{\rho}\widetilde{u}_1\widetilde{u}_1$$

$$\overline{F}_{\mathrm{M},1} = (1-\overline{\rho})\widetilde{u}_1$$

$$\overline{Q}_{\mathrm{H}} = \overline{\rho}\frac{\omega_C}{\rho^2}\frac{\partial \rho}{\partial C}$$

Acoustic Source Term Distribution

Different locations of major source term contributions

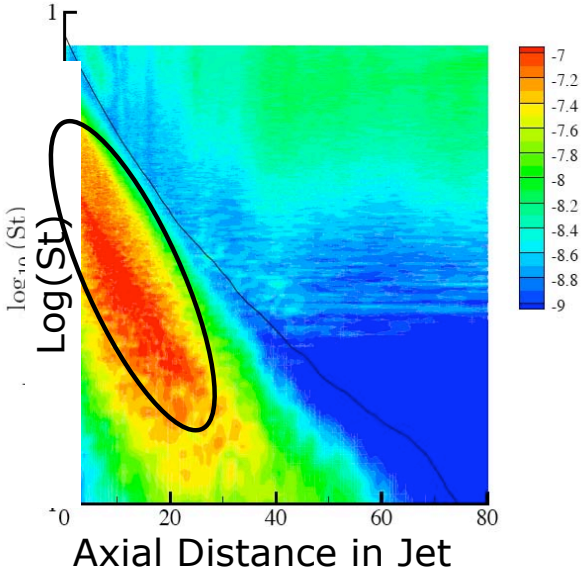

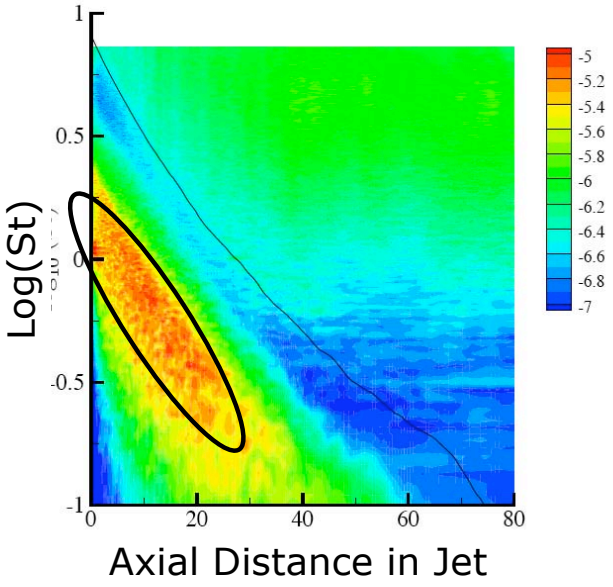

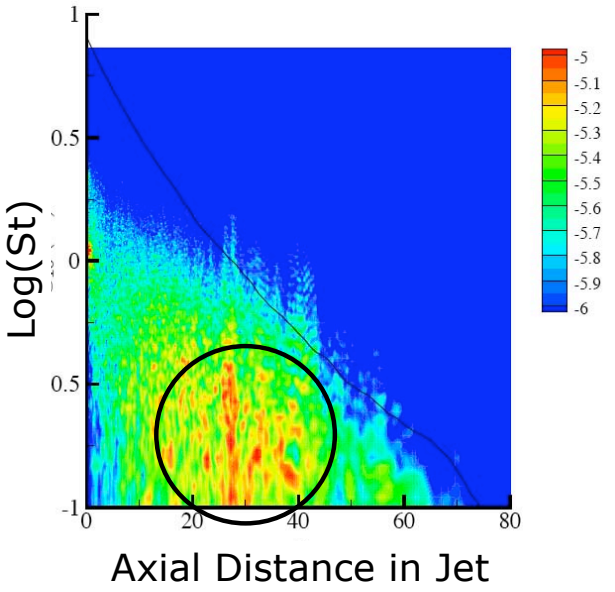

$$\overline{T}_{\mathrm{R},11} = \overline{\rho}\widetilde{u}_1\widetilde{u}_1$$

$$\overline{F}_{\mathrm{M},1} = (1-\overline{\rho})\widetilde{u}_1$$

$$\overline{Q}_{\mathrm{H}} = \overline{\rho}\frac{\omega_C}{\rho^2}\frac{\partial \rho}{\partial C}$$

Far-field Spectra

- Far-field sound pressure level

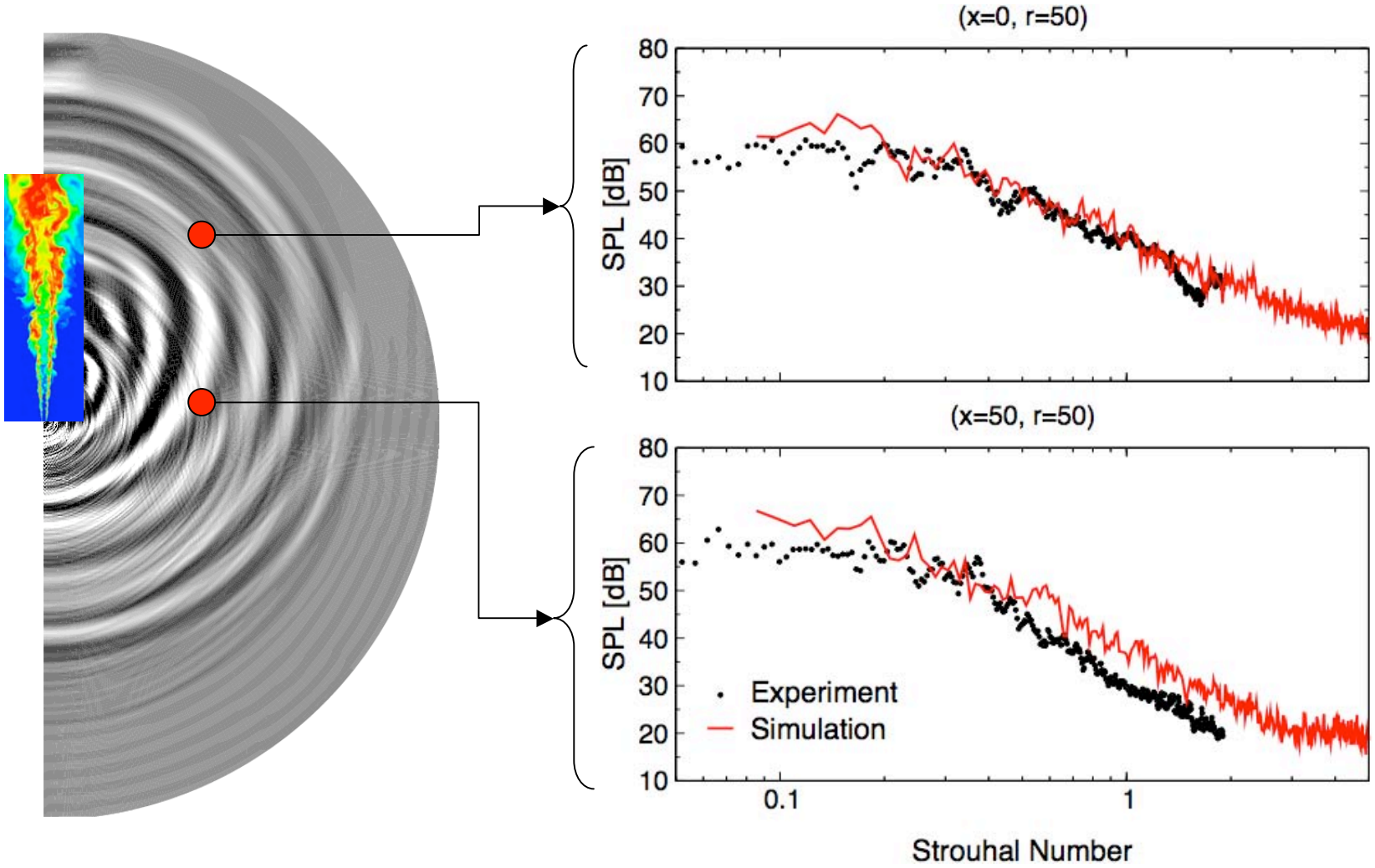

Combustion-Generated Noise

- Source term contributions

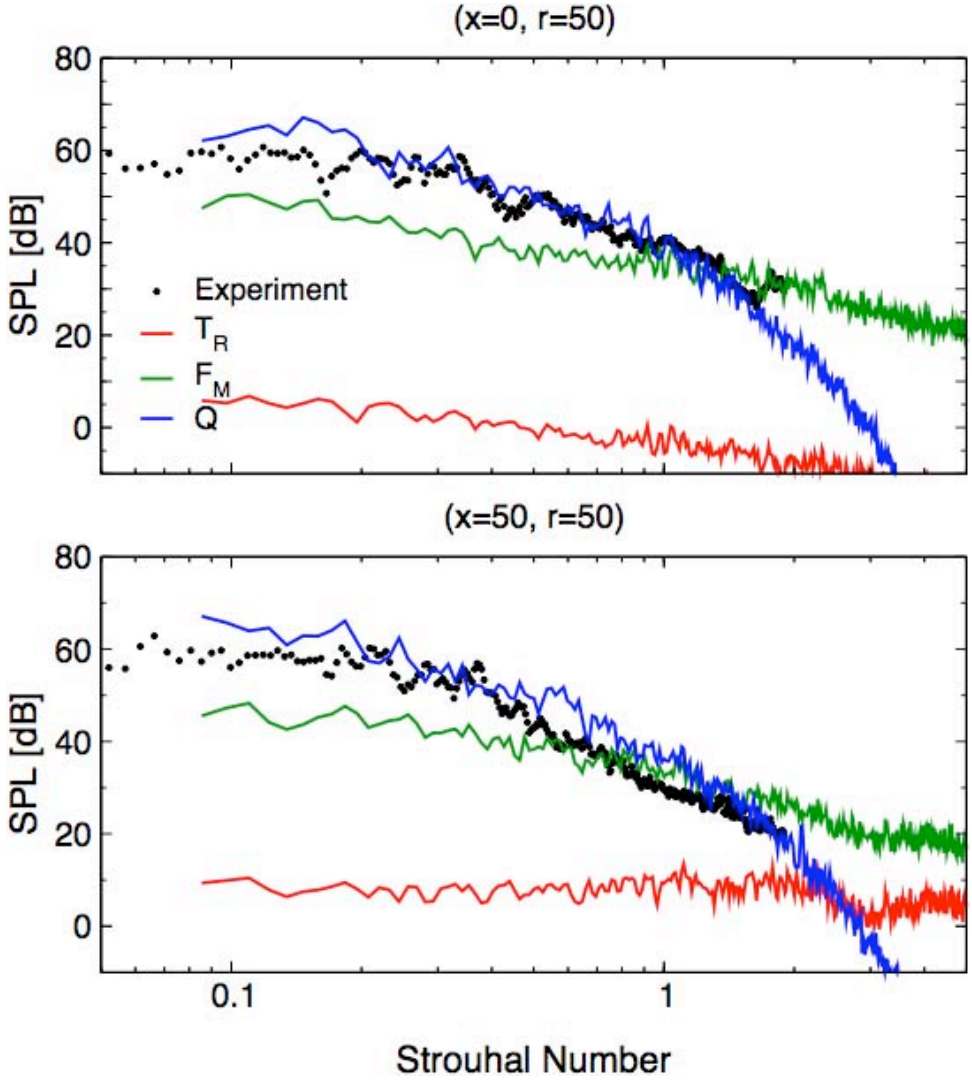

Directivity

- Directivity pattern: R = 100 diameters

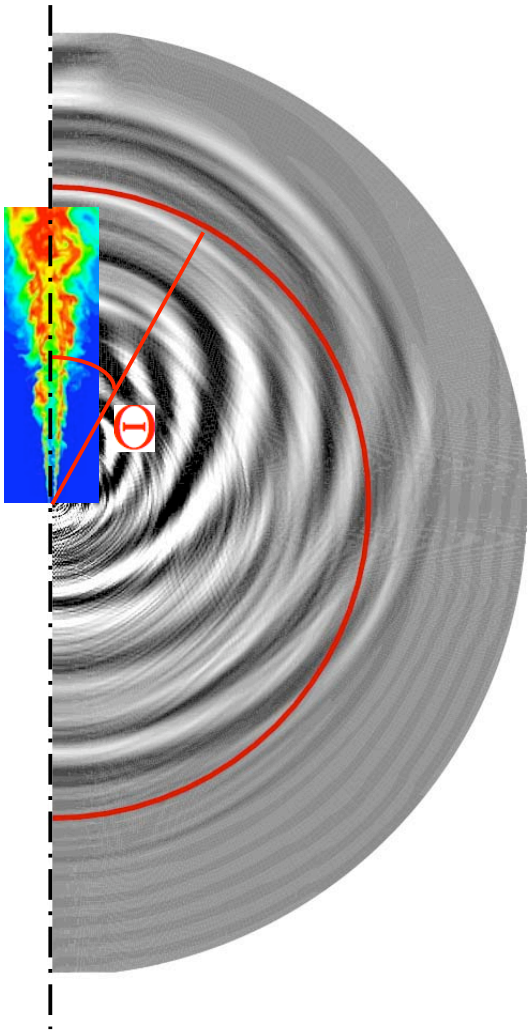

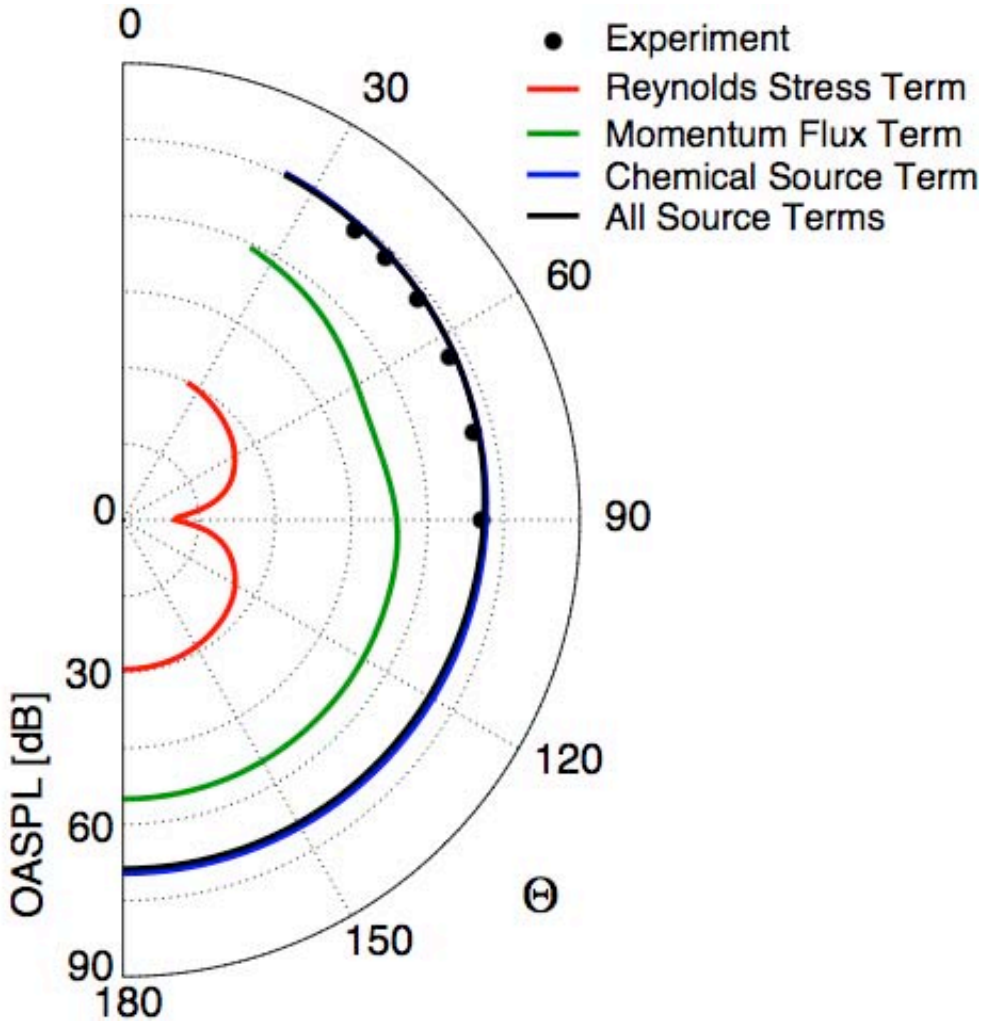

Summary of Open Flame Results

- Development of methodology for prediction of combustion-generated noise
  - Hybrid CLES/CAA approach using Lighthill's acoustic analogy and flamelet/progress variable model
- LES of DLR flame A (methane/hydrogen flame)
  - Good agreement of simulation with experiment for flow field quantities (velocity, mixture fraction) and chemical species
- Acoustic results
  - Identification of spurious noise sources
  - Different spatial extent of source terms
  - Momentum fluctuation term and Reynolds stress term negligible over chemical source term
  - Directivity pattern indicates monopole characteristics
- Results are nice, but …

Towards Noise Predictions in Complex Geometries

- CLES/LAA results cannot be used for more complex cases
- Computation of indirect noise not possible
- Test both options
  - Fully compressible
  - Goldstein's acoustic analogy
- Both options require high numerical accuracy

Aircraft engine combustor simulations using collocated scheme

Data for collocated scheme issued from **T. Colonius and S. K. Lele**, Progress in Aero. Sci. 40 (2004)

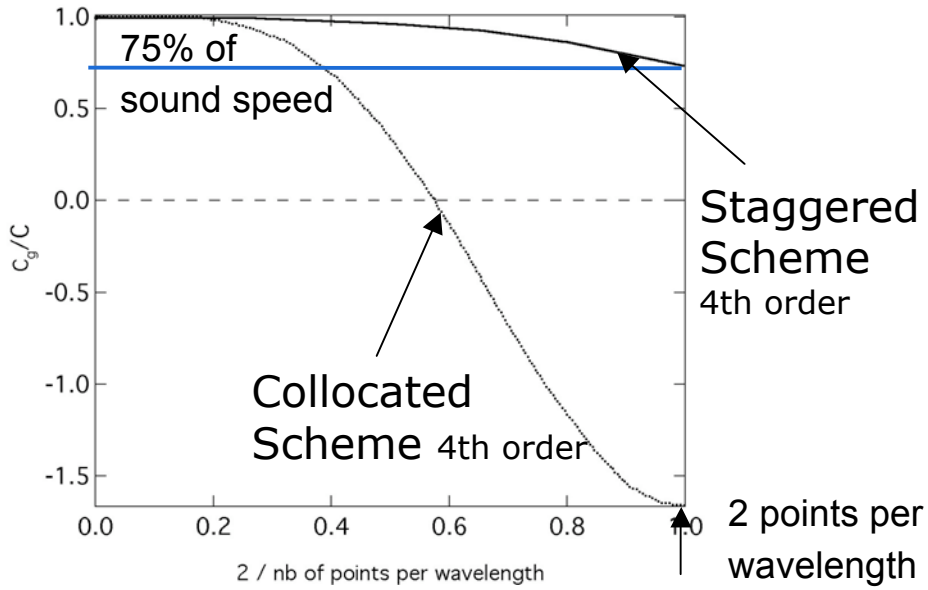

How to Achieve Adequate Accuracy in Complex Geometry Simulations?

Choices

- Unstructured mesh
  - Good geometry representation
  - Limited accuracy of numerical schemes
- Structured mesh
  - Very accurate
  - Staggered variable arrangement
  - Geometry representation difficult

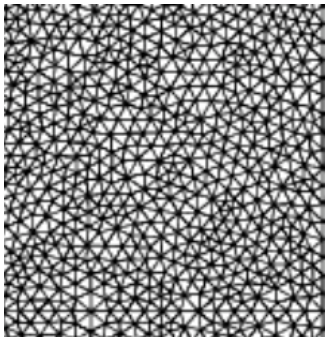

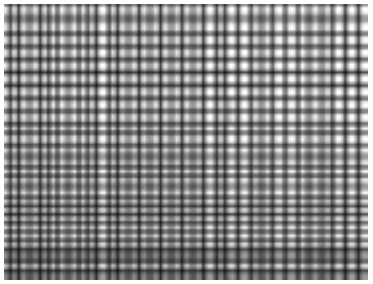

Tests show that staggered higher order schemes are required

Structured solver with immersed boundary method for geometry representation

LES Flow Solver

NGA Flow Solver (Desjardin, Blanquart, Pitsch, JCP, submitted)

- Structured mesh
- DNS/LES
- Staggered variable arrangement
- Arbitrary order of accuracy
- Energy conserving
- Geometry representation using immersed boundary method
- Compressible formulation underway
- Same code used for Goldstein equation solver

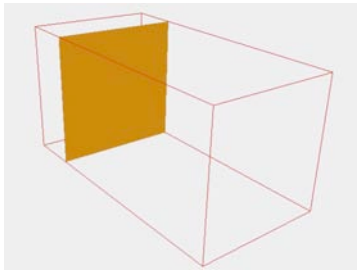

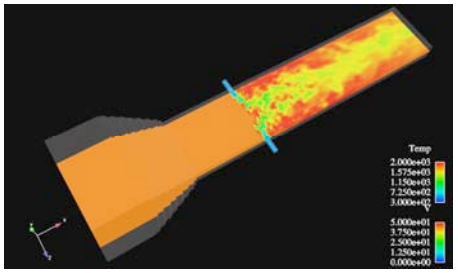

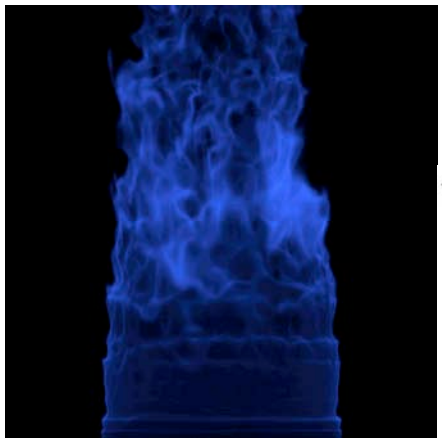

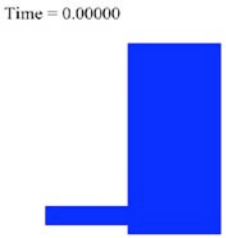

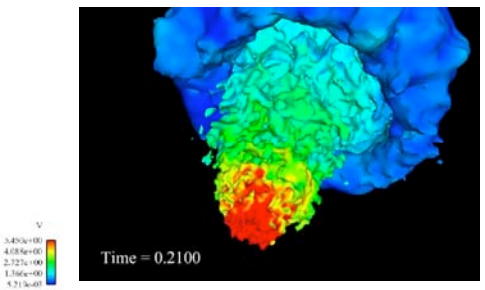

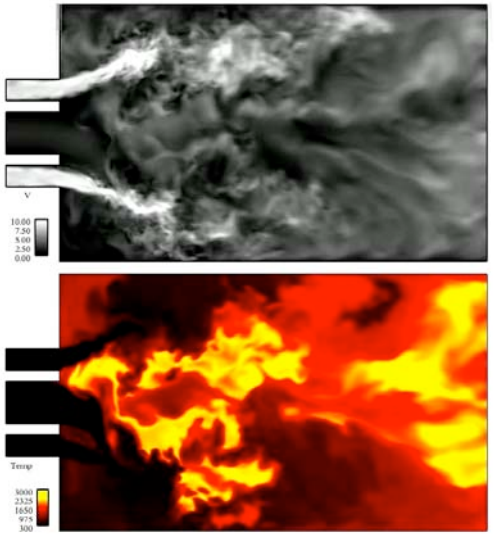

Immersed Boundary Method

- Start with stair-step representation of geometry
- Detect cells neighboring actual surface
- In these cells reconstruct velocities based on
  - Surface location + normals
  - Higher order interpolation

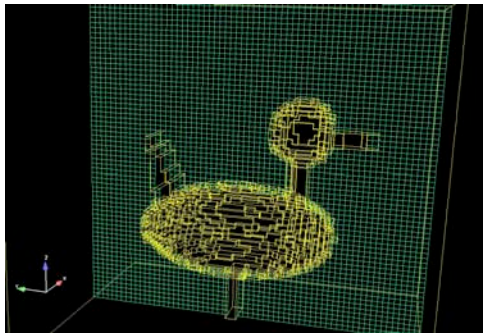

Stair step description

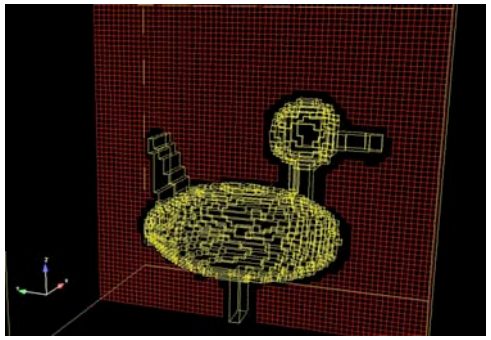

Neighbors detection
for interpolation

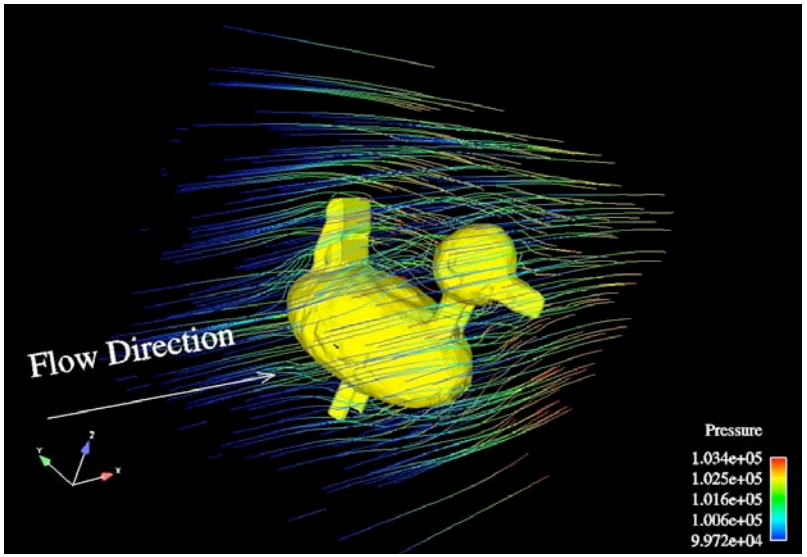

Compressible Solver Selection

Compressible NS equations:

$$\frac{\partial \rho}{\partial t} + \frac{\partial \rho u_j}{\partial x_j} = 0 \qquad P = \rho \frac{R}{W} T$$

$$\frac{\partial \rho u_i}{\partial t} + \frac{\partial \rho u_i u_j}{\partial x_j} = -\frac{\partial p}{\partial x_i} + \frac{\partial \tau_{ij}}{\partial x_j}$$

$$\frac{\partial \rho E}{\partial t} + \frac{\partial (\rho E + p) u_j}{\partial x_j} = \frac{C_p}{\Pr} \frac{\partial \mu T}{\partial x_j \partial x_j} + \frac{\partial \tau_{ij} u_i}{\partial x_j}$$

Two methods tested in 1D code:

- **Fractional step** (Moureau and Pitsch JCP, 2007)
  FV, 2nd order collocated, semi-implicit, low mach, low computational cost
- **Predictor-corrector** (Hou and Mahesh, JCP, 2005)
  FV, staggered in time, collocated in space, fully implicit, higher computational cost

Principle of fractional step method:

Characteristic splitting of convective and acoustic time scales

$$\frac{\bar{\phi}^* - \bar{\phi}^n}{\Delta t} + \nabla \cdot \left(\bar{\phi} \tilde{u} \right) - \bar{\phi} \nabla \cdot \tilde{u} = D_\phi$$

(1) Advection of conservative variables with convective velocity

$$\nabla \cdot \nabla \left(\delta \bar{P} \right) - \nabla \cdot \left\{ \frac{2\tilde{u}}{c^2 \Delta t} \delta \bar{P} \right\} - \frac{4}{c^2 \Delta t^2} \delta \bar{P} =$$

$$-\nabla \cdot \nabla \left(\bar{P}^* + \bar{P}^n \right) + \frac{4}{\Delta t} \left\{ \frac{\bar{\rho}^* - \bar{\rho}^n}{\Delta t} + \nabla \cdot \left\{ \frac{\bar{\rho}\tilde{u}^* + \bar{\rho}\tilde{u}^n}{2} \right\} \right\}$$

(2) Solve Helmholtz equation for pressure

Principle of predictor corrector method:

Iterative approach to solve continuity, momentum and energy

Uses trapezoidal rule to express pressure gradient term

$$\bar{p}^t = \frac{p^{t-\frac{1}{2}} + 2p^{t+\frac{1}{2}} + p^{t+\frac{3}{2}}}{4}$$

Introduce the corrected velocity and momentum in the energy equation to obtain the pressure correction

$$P^{3/2,k+1} = P^{3/2,k} + \delta p$$

$$u_i^{t+1,k+1} = u_i^* - \frac{\Delta t}{4\rho^{t+1}} \frac{\partial \delta p}{\partial x_i}$$

$$(u_i u_i)^{t+1,k+1} = u_i^* u_i^* - \frac{\Delta t}{2\rho^{t+1}} \frac{\partial \delta p}{\partial x_i} u_i^* + O(\delta p^2)$$

Compressible Solver Selection

Compressible NS equations:

$$\frac{\partial \rho}{\partial t} + \frac{\partial \rho u_j}{\partial x_j} = 0 \qquad P = \rho \frac{R}{W} T$$

$$\frac{\partial \rho u_i}{\partial t} + \frac{\partial \rho u_i u_j}{\partial x_j} = -\frac{\partial p}{\partial x_i} + \frac{\partial \tau_{ij}}{\partial x_j}$$

$$\frac{\partial \rho E}{\partial t} + \frac{\partial (\rho E + p) u_j}{\partial x_j} = \frac{C_p}{\Pr} \frac{\partial \mu T}{\partial x_j \partial x_j} + \frac{\partial \tau_{ij} u_i}{\partial x_j}$$

Two methods tested in 1D code:

- **Fractional step** (Moureau and Pitsch JCP, 2007)
  FV, 2nd order collocated, semi-implicit, low mach, low computational cost
- **Predictor-corrector** (Hou and Mahesh, JCP, 2005)
  FV, staggered in time, collocated in space, fully implicit, higher computational cost

Principle of fractional step method:

Characteristic splitting of convective and acoustic time scales

$$\frac{\bar{\phi}^* - \bar{\phi}^n}{\Delta t} + \nabla \cdot \left(\bar{\phi} \tilde{u} \right) - \bar{\phi} \nabla \cdot \tilde{u} = D_\phi$$

(1) Advection of conservative variables at convective velocity

$$\nabla \cdot \nabla \left(\delta \bar{P} \right) - \nabla \cdot \left\{ \frac{2\tilde{u}}{c^2 \Delta t} \delta \bar{P} \right\} - \frac{4}{c^2 \Delta t^2} \delta \bar{P} =$$

$$-\nabla \cdot \nabla \left(\bar{P}^* + \bar{P}^n \right) + \frac{4}{\Delta t} \left\{ \frac{\bar{\rho}^* - \bar{\rho}^n}{\Delta t} + \nabla \cdot \left\{ \frac{\bar{\rho}\tilde{u}^* + \bar{\rho}\tilde{u}^n}{2} \right\} \right\}$$

(2) Resolution of Helmhotlz equation for pressure

Principle of predictor corrector method:

Iterative approach to solve continuity, momentum and energy

Uses trapezoidal rule to express pressure gradient term

$$\bar{p}^t = \frac{p^{t-\frac{1}{2}} + 2p^{t+\frac{1}{2}} + p^{t+\frac{3}{2}}}{4}$$

Kinetic energy conserving

$$P^{3/2,k+1} = P^{3/2,k} + \delta p$$

$$u_i^{t+1,k+1} = u_i^* - \frac{\Delta t}{4\rho^{t+1}} \frac{\partial \delta p}{\partial x_i}$$

$$(u_i u_i)^{t+1,k+1} = u_i^* u_i^* - \frac{\Delta t}{2\rho^{t+1}} \frac{\partial \delta p}{\partial x_i} u_i^* + O(\delta p^2)$$

Predictor Corrector Method - On Staggered Grids

$$P^{3/2,k+1} = P^{3/2,k} + \delta p$$

$$u_i^{t+1,k+1} = u_i^* - \frac{\Delta t}{4\rho^{t+1}} \frac{\partial \delta p}{\partial x_i}$$

$$(u_i u_i)^{t+1,k+1} = u_i^* u_i^* - \frac{\Delta t}{2\rho^{t+1}} \frac{\partial \delta p}{\partial x_i} u_i^* + \mathrm{O}(\delta p^2)$$

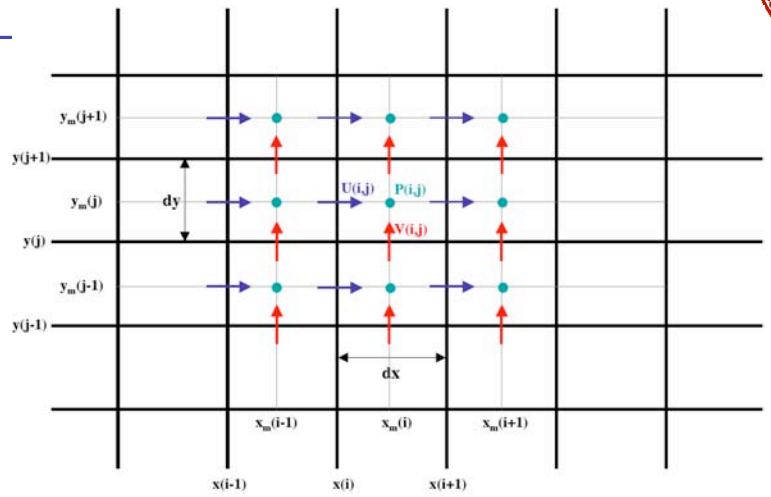

$$\frac{1}{2\Delta t}\delta p - \frac{\gamma-1}{4}\overline{\rho^{t+1}}^{t}\left(\overline{\frac{\partial \delta p}{\partial x_i}\frac{1}{\overline{\overline{\rho^{t+1}}^{xi}}^{t}}}^{xi}\right)\overline{u_i^*}^{xi} + \frac{\partial}{\partial x_j}\left\{\frac{\gamma}{4}\overline{\delta p}^{xj} u_j^{t+\frac{1}{2},*}\right\}$$

Linearized energy equation

$$-\frac{\partial}{\partial x_j}\left\{\frac{\gamma}{2}\overline{\overline{p}^{t}}^{xj}\frac{\Delta t}{4\overline{\overline{\rho^{t+1}}^{xj}}^{t}}\frac{\partial \delta p}{\partial x_j}\right\} - \frac{\gamma-1}{2}\frac{\partial}{\partial x_j}\left\{\overline{\rho^{t+\frac{1}{2}}}^{xj}\overline{u_i^{t+\frac{1}{2},*}}^{xj}\overline{u_i^{t+\frac{1}{2},*}}^{xj}\frac{\Delta t}{8\overline{\overline{\rho^{t+1}}^{xj}}^{t}}\frac{\partial \delta p}{\partial x_j}\right\} - \frac{\gamma-1}{2}\frac{\partial}{\partial x_j}\left\{\overline{\rho^{t+\frac{1}{2}}}^{xj}\Delta t\left(\overline{\frac{1}{4\overline{\overline{\rho^{t+1}}^{xi}}^{t}}\frac{\partial \delta p}{\partial x_i}}^{xj}\right)\overline{u_i^{t+\frac{1}{2},*}}^{xj} u_j^{t+\frac{1}{2},*}\right\}$$

$$= -\frac{1}{2\Delta t}\left(p^{t+\frac{3}{2},k} - p^{t-\frac{1}{2}}\right) - \frac{\gamma-1}{2\Delta t}\left[\overline{\rho^{t+1}}^{t}\overline{u_i^*}^{xi}\overline{u_i^*}^{xi} - \overline{\rho^{t}}^{t}\overline{u_i^{t}}^{xi}\overline{u_i^{t}}^{xi}\right] - \frac{\partial}{\partial x_j}\left\{\gamma\overline{\overline{p}^{t}}^{xj} u_j^{t+\frac{1}{2},*} + \frac{\gamma-1}{2}\overline{\rho^{t+\frac{1}{2}}}^{xj}\overline{u_i^{t+\frac{1}{2},*}}^{xj}\overline{u_i^{t+\frac{1}{2},*}}^{xj} u_j^{t+\frac{1}{2},*}\right\}$$

$$+(\gamma-1)\frac{\partial}{\partial x_j}\left\{\overline{\overline{\tau_{ij}}^{t}}^{t}\overline{u_i}^{t}\right\} + \frac{C_p}{\mathrm{Pr}}(\gamma-1)\frac{\partial}{\partial x_j}\left\{\overline{\mu}^{xj}\frac{\partial T^{t+\frac{1}{2},k}}{\partial x_j}\right\}$$

Verification Tests

Wave propagation (1D), Pulse (1D), Taylor vortex (2D), Pulse (2D) periodic BC

Computational efficiency

CASE	Grid points	Bicgstab	Sub iterations	Pressure residual
WAVE	64	2	4	1e-11
PULSE	32	6, 3, 2	4	1e-9
VORTEX	64 x 64	4	4	1e-8

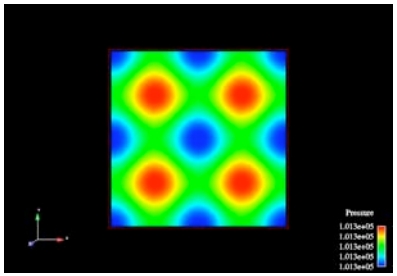

Taylor vortex

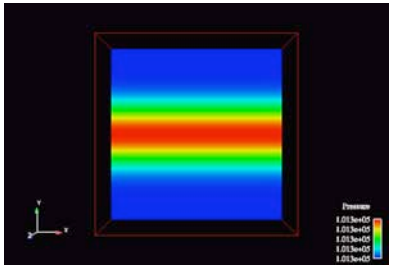

Pulse propagation, y

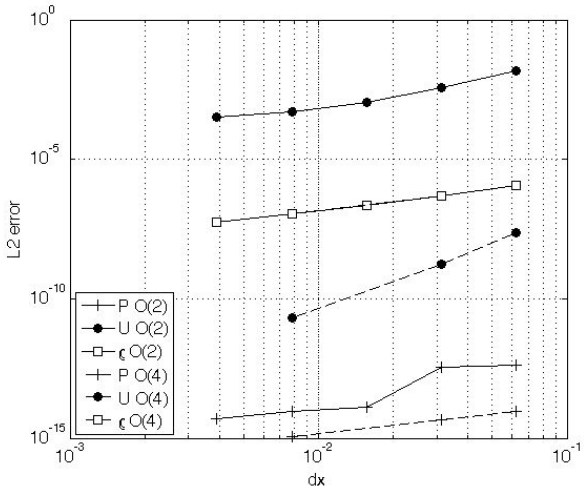

Spatial accuracy, second and fourth order of the spatial deriatives

Second order

Fourth order

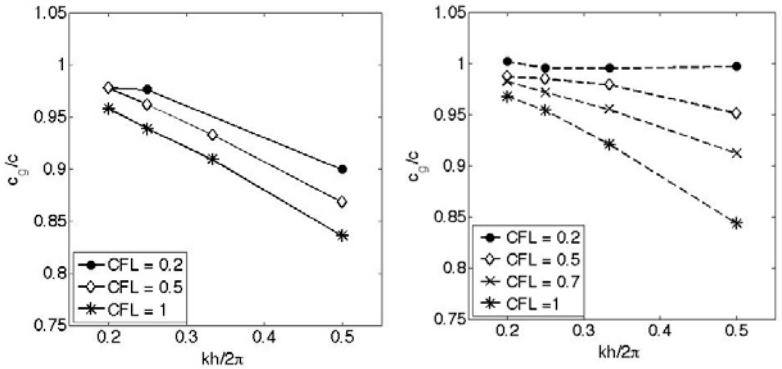

Evolution of the normalized speed of sound as a function of the number of grid points per period and acoustic CFL number

Numerical Accuracy Requirement and Resolution Verification: 'Combustor - Type Test Case'

How many wave reflections can be propagated accurately in the domain based on this limit frequency?

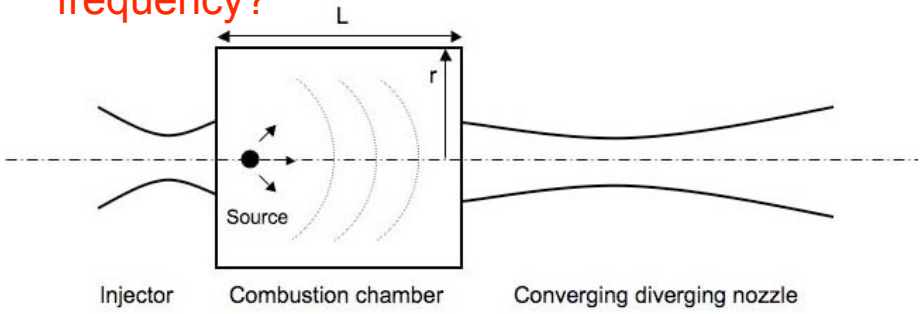

Interesting frequencies are less than 5000 Hz

Wavelength range, based on a limit frequency of 10 000 Hz: $\lambda = c / f$

Non reactive configuration

$c = 346 \ \ m/s$

$T = 298 \ \ K$

$\rho = 1.18 \ \ kg/m^3$

$\lambda_c = 0.0347 \ \ m$

Reactive configuration

$c = 897 \ \ m/s$

$T = 2000 \ \ K$

$\rho = 0.17 \ \ kg/m^3$

$\lambda_h = 0.0897 \ \ m$

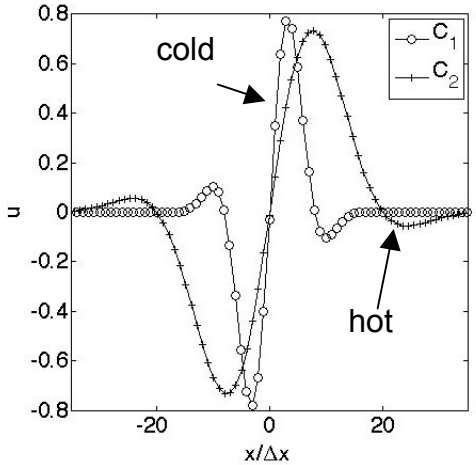

Initial signals

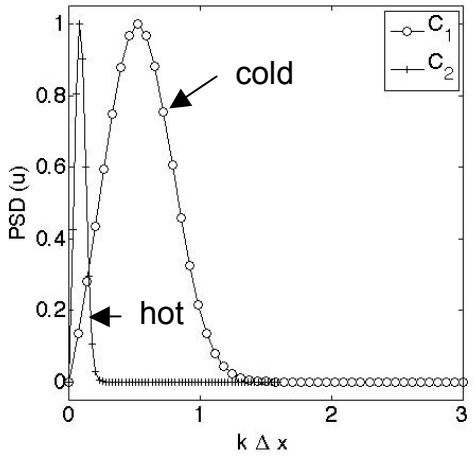

Initial signals power density spectra

$$u(x) = \sin\left(\frac{2\pi x}{a\Delta x}\right)\exp\left[-\ln 2\left(\frac{x}{b\Delta x}\right)^2\right]$$

a is set to have 16 points per dominant wavelength in the cold case. This gives around 41 points per dominant wavelength in the reactive case.

Numerical Accuracy Requirement and Resolution Verification: 'Combustor - Type Test Case'

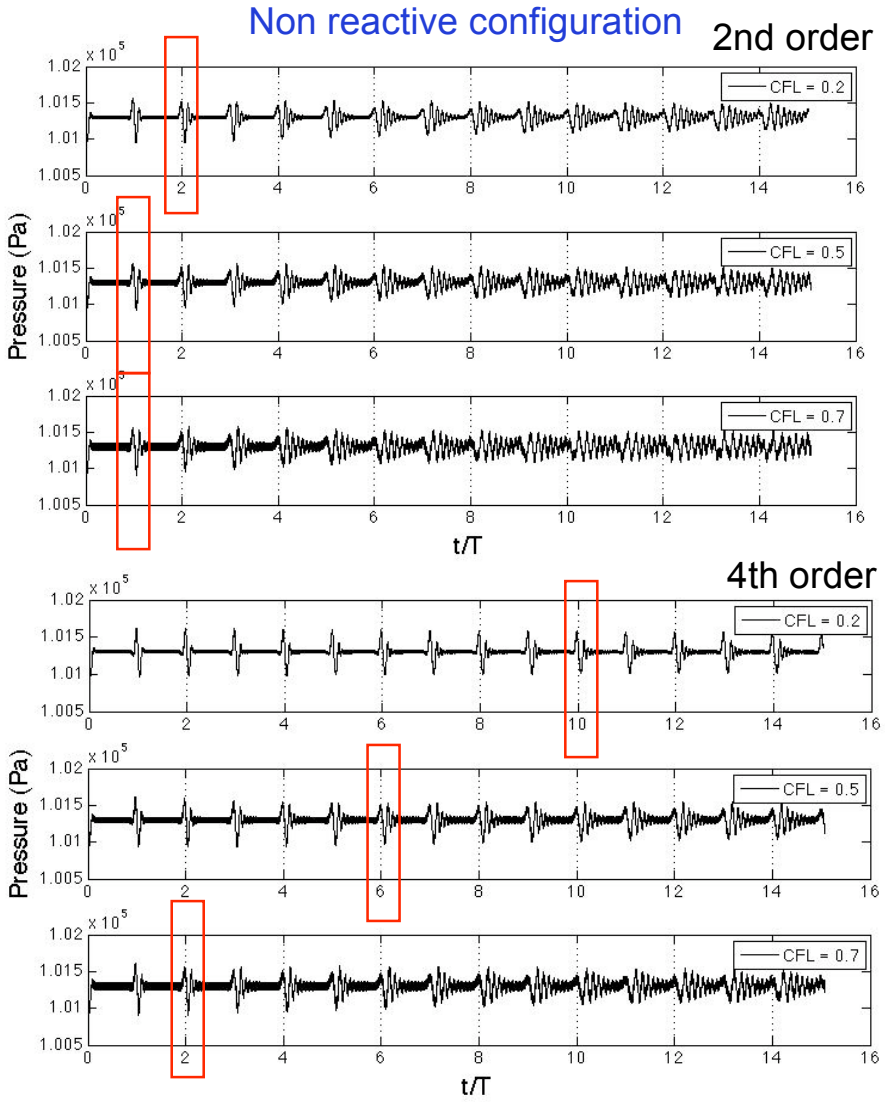

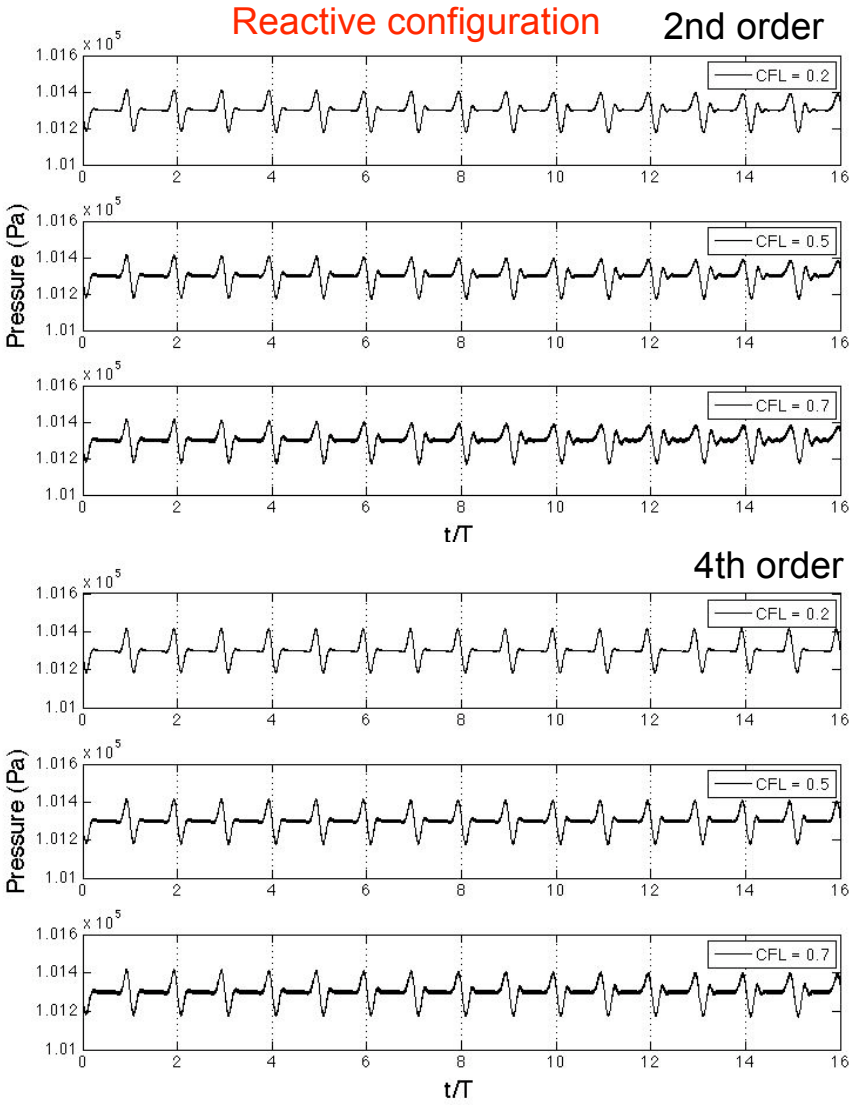

Fourth order: 10 reflections, with low CFL number

Fourth order: 14 reflections, with low CFL number

Numerical Accuracy Requirement and Resolution Verification: 'Combustor - Type Test Case'

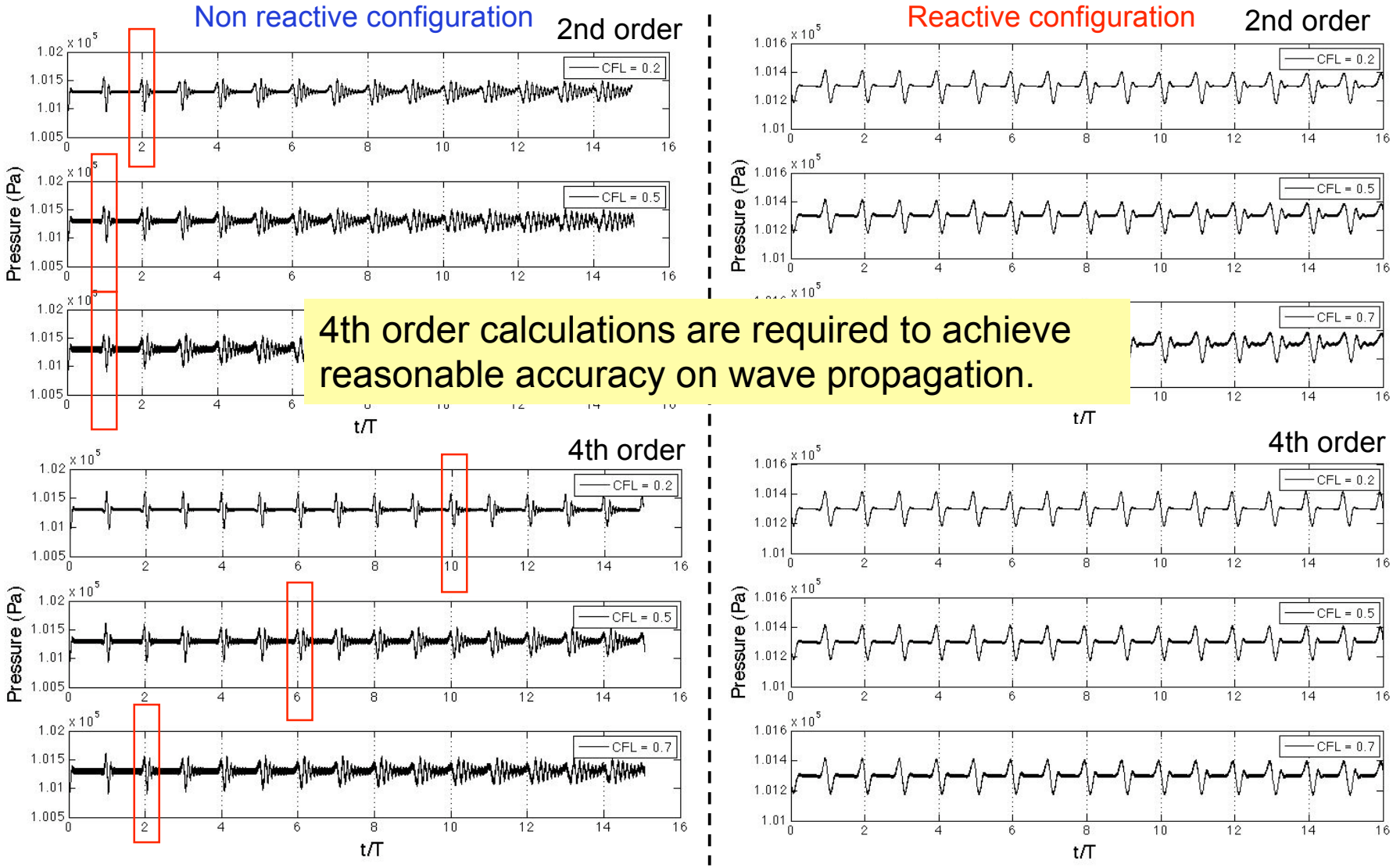

Fourth order: 10 reflections, with low CFL number

Fourth order: 14 reflections, with low CFL number

Goldstein's Acoustic Analogy

Introduce effects of combustion into Goldstein equations:

- In reaction zone, large fluctuations of ratio of specific heat
- Heat release fluctuation (Direct sound source)

$$\overline{\rho}\frac{\overline{D}}{Dt}\frac{\rho'}{\overline{\rho}} + \frac{\partial}{\partial x_j}\overline{\rho}u_j' = 0\,, \qquad \textbf{Density}$$

$$\overline{\rho}\left(\frac{\overline{D}}{Dt}u_i' + u_j'\frac{\partial \tilde{v}_i}{\partial x_j}\right) + \frac{\partial}{\partial x_i}p_e' - \frac{\rho'}{\overline{\rho}}\frac{\partial}{\partial x_j}\tilde{\tau}_{ij} = \frac{\partial}{\partial x_j}(e_{ij}' - \tilde{e}_{ij})\,, \qquad \textbf{Velocity}$$

$$\begin{aligned}\frac{\overline{D}}{Dt}(\overline{\beta}-1)p_e' + \overline{\beta}p_e'\frac{\partial \tilde{v}_j}{\partial x_j} + \gamma\frac{\partial}{\partial x_j}\overline{\rho C_p T}u_j' - u_i'\frac{\partial \tilde{\tau}_{ij}}{\partial x_j} \qquad \textbf{Total energy}\\ = \frac{\partial}{\partial x_j}(\eta_j' - \tilde{\eta}_j) + (e_{ij}' - \tilde{e}_{ij})\frac{\partial \tilde{v}_i}{\partial x_j}\underbrace{-D_0\alpha' + \dot{\omega}_T'}_{\textbf{New terms}}\,,\end{aligned}$$

$$\eta_i' = -\rho v_i' h_0' - q_i' + \sigma_{ij}v_j'$$

$$\tilde{\eta}_i = -\overline{\rho}\left(\widetilde{h_0 v_i} - \tilde{h}_0\tilde{v}_i\right) + v_i\sum_j \frac{1}{2}\overline{\rho}\left(\widetilde{v_j^2} - \tilde{v}_j^{\,2}\right)$$

Numerical Scheme and Accuracy

Use explicit, staggered solver for reactive Goldstein's equations

- Because of multiple reflections inside a realistic domain, propagation of acoustic wave has to be accurate
- 6^{th} order in space and time is good compromise between accuracy and efficiency
- Good propagation properties for waves with more than 8 points per wavelength

Propagation test defined by Bogey and Bailly (JCP,2004)

8 points per wave

L2 error < 20% after 10 turnover times

Spatial discretization

... 4th (CFL=0.5), — 6th (CFL=1.0)

• Exact solution

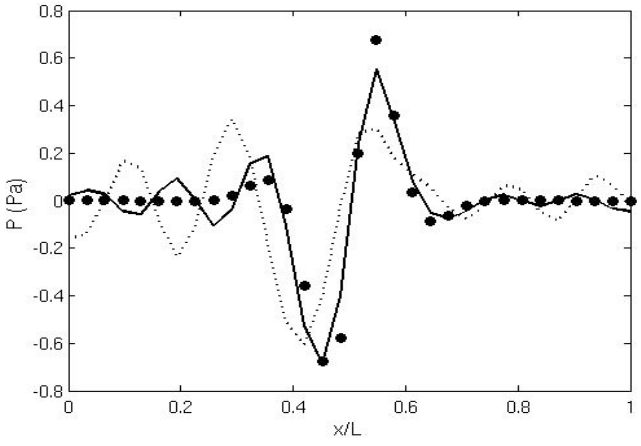

Temporal discretization

... 4 RK steps, — 6 RK steps

• Exact solution

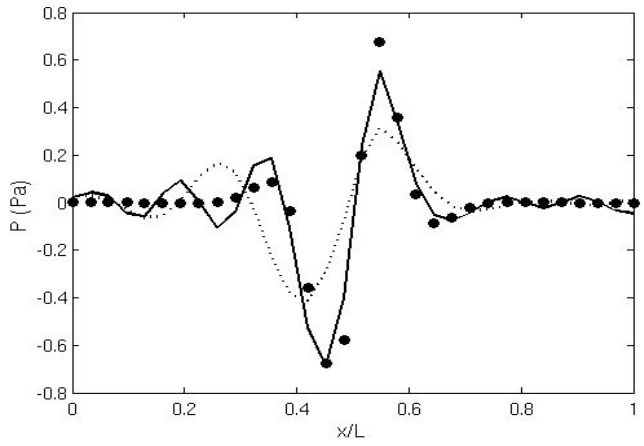

Numerical Noise and Explicit Filtering

- Waves with less than 8 points per wavelength are not well propagated
- Must be damped to avoid any numerical noise

- Use of explicit filtering of the fields
- Does not influence propagation of well resolved waves

Selective filter defined by Bogey and Bailly (JCP,2004)

Only damps waves with less than 4 points per wavelength

4 points/wavelength

... Non-filtered, — Filtered

• Exact solution

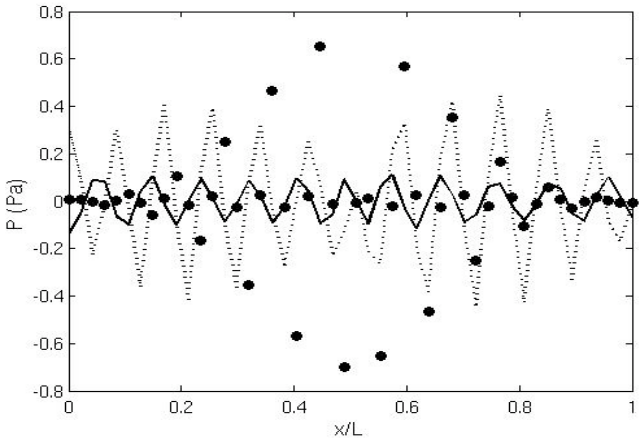

8 points/wavelength

... Non-filtered, —Filtered

• Exact solution

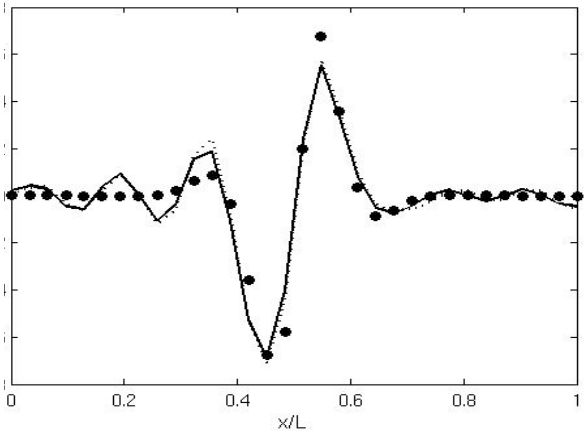

Conclusions

- Presented strategy to do combustion noise simulations for jet engines
  - Fully compressible
  - Goldstein's acoustic analogy
- Test accuracy of combustion model and associated numerics in open flame using CLES/LAA
  - Errors from quantities in chemistry tabulation being under-resolved on computational mesh
  - Errors in interpolation in chemistry table
- Good results compared with experimental data for
  - Flow field and scalars
  - Sound pressure level
- Towards complex geometry
  - Fully compressible solver needs staggered 4^{th} order accurate scheme
  - Needs structured mesh
  - Similar accuracy required for for solving acoustic analogy